

Quantum rings for beginners: Energy spectra and persistent currents

S. Viefers¹, P. Koskinen², P. Singha Deo³, and M. Manninen²

¹*Department of Physics, University of Oslo, P.O. Box 1048 Blindern, N-0316 Oslo, Norway*

²*Department of Physics, University of Jyväskylä, FIN-40351 Jyväskylä, Finland and*

³*S.N. Bose National Centre for Basic Sciences, JD Block, Sector III, Salt Lake City, Kolkata 98, India*

(Dated: October 29, 2018)

Theoretical approaches to one-dimensional and quasi-one-dimensional quantum rings with a few electrons are reviewed. Discrete Hubbard-type models and continuum models are shown to give similar results governed by the special features of the one-dimensionality. The energy spectrum of the many-body states can be described by a rotation-vibration spectrum of a 'Wigner molecule' of 'localized' electrons, combined with the spin-state determined from an effective antiferromagnetic Heisenberg Hamiltonian. The persistent current as a function of the magnetic flux through the ring shows periodic oscillations arising from the 'rigid rotation' of the electron ring. For polarized electrons the periodicity of the oscillations is always the flux quantum Φ_0 . For nonpolarized electrons the periodicity depends on the strength of the effective Heisenberg coupling and changes from Φ_0 first to $\Phi_0/2$ and eventually to Φ_0/N when the ring gets narrower.

PACS numbers: 73.23.Ra, 73.21.Hb, 75.10.Pq, 71.10.Pm

I. INTRODUCTION

The observation of the Aharonov-Bohm oscillations[1] and persistent current[2] in small conducting rings, on one hand, and the recent experimental developments in manufacturing quantum dots[3] and rings[4] with only a few electrons, on the other, have made quantum rings an ever increasing topic of experimental research and a new playground for many-particle theory in quasi-one-dimensional systems.

Many properties of the quantum rings can be explained with single-electron theory, which in a strictly one-dimensional (1D) system is naturally very simple. On the contrary, the many-particle fermion problem in 1D systems is surprisingly complicated due to enhanced importance of the Pauli exclusion principle. In general, correlations are always strong, leading to non-fermionic quasiparticles as low energy excitations. It is then customary to say that strictly 1D systems are not 'Fermi liquids' but 'Luttinger liquids' with specific collective excitations (for reviews see[5, 6, 7, 8]).

The many-particle approach normally used in studying the properties of Luttinger liquids starts by assuming an infinitely long strictly one-dimensional system. In small finite rings a direct diagonalization of the many-body Hamiltonian, using numerical techniques and a suitable basis, is possible and can provide more direct information on the many-particle states. Two different theoretical models have been used for the finite rings. In a *discrete model* the ring is assumed to consist of L discrete lattice sites (or atoms) with N electrons, which can hop from site to site. In this case the electron-electron interaction is usually assumed to be effective only when the electrons are at the same site. The many-particle Hamiltonian is then a Hubbard Hamiltonian[9] or its extension. Another possibility is to assume a ring-shaped smooth external confinement where interacting electrons move. In this

continuum model the electron-electron interaction is usually the normal Coulomb interaction ($e^2/4\pi\epsilon_0 r$). In the case of a small number of electrons (typically $N < 10$) the many-particle problem is well defined in both models and can be solved with numerical diagonalization techniques for a desired number of lowest energy states.

Other many-particle methods have also been applied for studying the electronic structure of quantum rings. The discrete rings can be solved by using the Bethe ansatz[10, 11], which becomes powerful especially in the case of an infinitely strong contact interaction (the so-called t -model). In the case of continuum rings, quantum Monte Carlo methods and density functional methods have been used (see Sec. XIII).

The purpose of this paper is to give an introductory review to the many-particle properties of rings with a few electrons. Our aim is not to give a comprehensive review of all the vast literature published. The main emphasis is to clarify the relations between different methods and to point out general features of the electronic structures of the rings and their origins. Most of the results we show in figures are our own computations made for this review. However, we want to stress that most of the phenomena shown have been published before, (in many case by several authors) and we will give reference to earlier work.

We take an approach where we analyse the many-body excitation spectrum and its relation to the single particle spectrum and electron localization along the ring. We will show that, irrespective of the model, the excitation spectrum in narrow rings can be understood as a rotation-vibration spectrum of localized electrons. The effect of the magnetic flux penetrating the ring is also studied as the change of the spectrum as a function of the flux. This is used to analyze the periodicity of the *persistent current* as a function of the flux. Again, it is shown that similar results are obtained with the discrete

and continuum models.

Throughout this paper we use the term “spinless electrons” to describe a system of completely polarized electron system, i.e. the many-particle state having maximum total spin and its z -component. We use lower case letters to describe single particle properties and capital letters for many-particle properties (e.g. m and M for angular momenta). We use terms like “rotational” and “vibrational” states quite loosely for describing excitations, which in certain limiting cases have exactly those meanings. When we talk about the rotational state we will use the terminology of the nuclear physics and call the lowest energy state of a given angular momentum an *grast* state.

Experimentally, the study of the spectra of quantum ring is still in an early state of an impressive development. It is not yet the time to make detailed comparison between the theory and experiments. Nevertheless, we will give in Sec. II a short overview of the experimental situation.

We then attempt to review the theory of quantum rings in a logical and pedagogical way, starting with the simplest case of non-interacting spinless fermions (Secs. III and IV) and classical interacting electrons (Sec. V), then introducing the effect of magnetic flux (Sec. VI) and spin (Sec. VII). Lattice models are presented in Secs. VIII and IX, followed by numerical approaches (Secs. X, XI, XIII). The periodicity properties of the many-body spectrum is discussed in Sec. XII. We also briefly discuss the relation of these previous approaches to the Luttinger liquid formalism (Sec. XIV), and introduce pair correlation functions as a tool to study the internal structure of the many-electron state (Sec. XV). Most of the review will deal with rings where the external magnetic flux penetrates the ring in such a way that the magnetic field is zero at the perimeter of the ring (Aharonov-Bohm flux) and the ring is free from impurities. Nevertheless, in Sections XVI and XVII we will give short overviews of the effects of the Zeeman splitting and impurities on the excitation spectrum.

Several interesting aspects of quantum rings will have to be neglected in this paper. Among these are the exciting possibilities of observing experimentally the spin Berry phase (see, however, Sec. II for a brief experimental overview) and, even more exotically, fractional statistics (anyons) [12].

II. EXPERIMENTAL SITUATION

Since the mid-eighties, there has been an impressive experimental development towards smaller and smaller 2D quantum rings; with the most recent techniques one has reached the true quantum limit of nanoscopic rings containing only a few electrons [4, 13, 14]. At the same time, many of the experiments still study mesoscopic rings with hundreds of electrons. Methods of forming such rings include lithographic methods for forming individual rings on

a semiconductor surface. The spectroscopic techniques are based on the tunneling current through the ring or capacitance spectroscopy. Another possibility is to create a large number of self-organized rings on a substrate. The large number of rings allows for observation of direct optical absorption.

One of the hallmarks in this field of research has been the experimental observation of the Aharonov-Bohm effect [1] or, equivalently, persistent currents. One of the main challenges in order to observe this purely quantum mechanical effect, has been to ensure phase coherence along the circumference of the ring. Early experiments in the eighties and nineties reported observations of Aharonov-Bohm oscillations and persistent currents in metallic (Au or Cu) rings [15, 16, 17] and in loops in GaAs heterojunctions, i.e. two-dimensional electron gas [18, 19, 20, 21, 22, 23, 24]. A related effect which has received recent theoretical [25, 26, 27, 28, 29] and experimental [30, 31, 32, 33] attention, is the occurrence of a spin Berry phase [34] in conducting mesoscopic rings. The simplest example of this topological effect [35] is the phase picked up by a spin $\frac{1}{2}$ which follows adiabatically an inhomogeneous magnetic field; the Berry phase is then proportional to the solid angle subtended by the magnetic field it goes through. It has been shown [27] that in 1D rings, a Berry phase may arise due to spin-orbit interactions. The first experimental evidence of Berry’s phase in quantum rings was reported in 1999 by Morpurgo *et al.* [30] who interpreted the splitting of certain peaks in Fourier spectra of AB oscillations as being due to this effect. Very recently, Yang *et al.* [33] observed beating patterns in the Aharonov-Bohm conductance oscillations of singly connected rings; these results are interpreted as an interference effect due to the spin Berry phase.

There is by now a vast literature on experiments on quantum rings, and in the remainder of this section we will just discuss a few selected papers which report measurements of the many-body spectra, as this is the main topic of this review.

Fuhrer *et al.* [36] used an atomic force microscope to oxidize a quantum ring structure on the surface of a AlGaAs-GaAs heterostructure. By measuring the conductance through the dot they could resolve the so-called addition energy spectrum (see e.g. [37]) as a function of the magnetic field. The energy levels in the ring and their oscillation as a function of the magnetic field could be explained with a single particle picture assuming small non-spherical disturbance for the ring. The ring had about 200 electrons.

Lorke *et al.* [4, 14, 38] have succeeded to produce a few electron quantum rings from self-assembled InAs dots on GaAs using suitable heat treating. They used far-infrared (FIR) transmission spectroscopy and capacitance-voltage spectroscopy to study the ground and excited many-body states. The ring radius was estimated to be $R_0 = 14$ nm and the confining potential strength $\hbar\omega_0 = 12$ MeV (the confining potential is assumed to be $\frac{1}{2}m^*\omega_0^2(r - R_0)^2$). Lorke *et al.* were able to

study the limit of one and two electrons in the ring. The experimental findings were in consistence with a single electron picture.

Warburton *et al.*[39] studied the photoluminescence from self-assembled InAs quantum rings at zero magnetic field. By using a confocal microscope and taking advantage of the fact that each ring had unique charging voltages they were able to measure the photoluminescence from a single quantum ring. The photoluminescence spectra show the effect of the Hund's rule of favouring parallel spins and other details of the spectra, for example the singlet-triplet splitting.

The periodicity $\Phi_0 = h/e$ of the persistent current predicted for normal metal (not superconducting) rings has been observed several times for semiconductor quantum rings[18, 19, 20, 21, 23]. Also observations of other periodicities, or higher harmonics, have been reported[24, 40] but they have been interpreted as effects of the nonperfectness of the rings. Very recently, the first observation of the inherent Φ_0/N periodicity, which should appear in perfect very narrow rings, was reported [41].

III. STRICTLY 1D-RING WITH NONINTERACTING SPINLESS ELECTRONS

The single particle Hamiltonian of an electron in a strictly 1D ring depends only on the polar angle φ

$$H = -\frac{\hbar^2}{2m_e R^2} \frac{\partial^2}{\partial \varphi^2}, \quad \psi_m(\varphi) = e^{im\varphi}, \quad (1)$$

where R is the ring radius, m_e the electron mass (or effective mass) and $m\hbar$ is the angular momentum. (Note that the direction of the angular momentum axis is always fixed in a 2D structure). The corresponding energy eigenvalues are

$$\epsilon_m = \frac{\hbar^2 m^2}{2m_e R^2}. \quad (2)$$

We will first study spinless electrons, or a polarised electron system, where each electron has a $S_z = \uparrow$. In the noninteracting case the many-body state is a single Slater determinant. The total angular momentum is

$$M = \sum_i^N m_i \quad (3)$$

and the total energy

$$E = \sum_i^N \epsilon_{m_i} \quad (4)$$

The lowest energy state for a given angular momentum, or the *yrast* state, is obtained by occupying single particle states consecutively (next to each other). This is due to the upwards curvature of ϵ_m . We will denote states

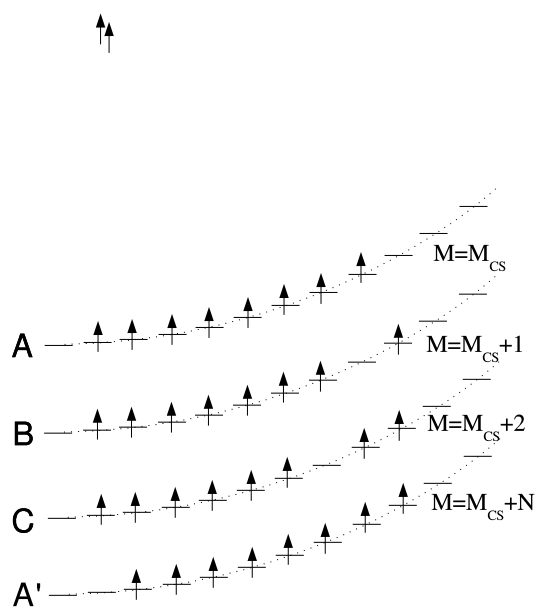


FIG. 1: Configurations of the many-body states of eight noninteracting electrons in a ring for spinless electrons. A and A' give local minima in the yrast line, while B and C correspond to 'vibrational excitations'.

consisting of single particle states with consecutive angular momenta, say from m_0 to $m_0 + N - 1$, as "compact states". These states have energy

$$E_{CS} = \frac{\hbar^2}{2m_e R^2} [Nm_0^2 + (N^2 - N)m_0 + \frac{1}{6}(2N^3 - 3N^2 + N)] \quad (5)$$

and the angular momentum

$$M = Nm_0 + \frac{N(N-1)}{2}. \quad (6)$$

It is interesting to note that while the single particle energy increases with the angular momentum as $\hbar^2 m^2 / 2m_e R^2$, the lowest many-body energy increases, in the limit of large M , as $\hbar^2 M^2 / 2(Nm_e)R^2$. An yrast state of the ring with N electrons corresponds then to a single particle with mass Nm_e . This is our first notion of "rigid rotation" of the quantum state.

The structure of the yrast states is illustrated schematically in Fig. 1, and the actual energy levels as a function of the angular momentum are shown in Fig. 2. Naturally, the compact states give local minima of the yrast spectrum. In what follows, the most important property of the many-particle states is that the *internal structure* of the state does not change when the angular momentum is increased by a multiple of N . (By the term "internal structure" of a state, we refer to interparticle correlations which can be seen by using a rotating frame, as discussed by Maksym in the case of quantum dots[42].) This follows from the notion that

$$\Psi_{M+\nu N}^{\text{Slater}}(\{\varphi_i\}) = \exp\left(i\nu \sum_i^N \varphi_i\right) \Psi_M^{\text{Slater}}(\{\varphi_i\}), \quad (7)$$

where ν is any integer. This kind of change of the total angular momentum corresponds to a rigid rotation of the

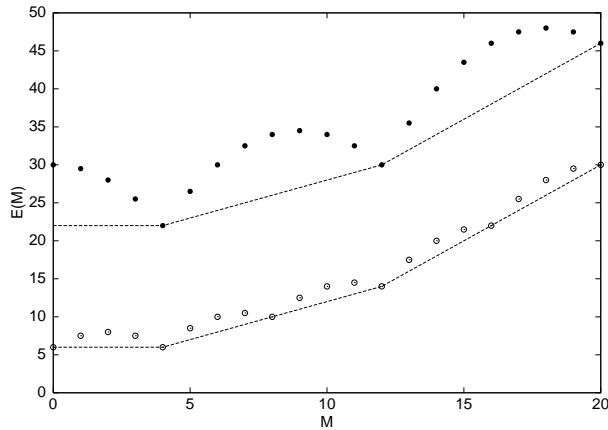


FIG. 2: The lowest total energy of eight noninteracting electrons as a function of the total angular momentum, i.e. the yrast line. Black dots: spinless electrons; open circles: electrons with spin. The local minima are connected with dashed lines.

state and naturally leads to the above mentioned result that the N -electron system rotates like a single particle with mass Nm_e . Moreover, correlation functions are the same for both $\Psi_{M+\nu N}^{\text{Slater}}$ and Ψ_M^{Slater} since they are derived from the square $|\Psi|^2$. Note that the minima of the yrast spectra occur at angular momenta $M = \nu N$ if N is odd and at angular momenta $M = \nu N + N/2$ if N is even.

IV. LOCALIZATION OF NONINTERACTING SPINLESS FERMIONS IN 1D

Classical noninteracting particles do not have phase transitions and are always in a gas phase: There is no correlation between the particles. In the quantum mechanical case, due to the Pauli exclusion principle, one-dimensional spinless fermions behave very differently: Two electrons can not be at the same point. This means that noninteracting spinless fermions are identical with fermions interacting with an infinitely strong delta-function interaction. The requirement that the wave function has to go to zero at points where electrons meet, increases the kinetic energy proportional to $1/d^2$ where d is the average distance between the electrons (this is analogous to the kinetic energy of a single particle in a one-dimensional potential box). The requirement of the wave function being zero in the contact points has the classical analogy that the electrons can not pass each other[7]. The pressure of the kinetic energy scales as an interparticle energy of the form $1/[R^2(\varphi_i - \varphi_j)^2]$, leading to the interesting result that the energy spectrum of the particles interacting with the δ -function interaction agrees with that of particles with $1/r^2$ interaction. In fact, the model of 1D particles with a $1/r^2$ interaction,

the so-called Calogero-Sutherland model[43, 44], is exactly solvable. We will return to this in Sec. IX E.

We will now demonstrate that the non-compact states may in fact be regarded as *vibrational* states. The simplest case is that with two electrons. The Slater determinant is (omitting normalization)

$$\psi_{m_1 m_2}(\varphi_1, \varphi_2) = e^{im_1 \varphi_1} e^{im_2 \varphi_2} - e^{im_1 \varphi_2} e^{im_2 \varphi_1}. \quad (8)$$

The square of the amplitude of this wave function can be written as

$$|\psi_{m_1 m_2}(\varphi_1, \varphi_2)|^2 = 4 \sin^2 \left[\frac{1}{2} (\Delta m \Delta \varphi) \right], \quad (9)$$

where $\Delta m = m_1 - m_2$ and $\Delta \varphi = \varphi_2 - \varphi_1$. This means that the maxima of this wave function occur at points $\Delta \varphi = (1 + 2n)\pi/\Delta m$ where n is an integer. The compact ground state has $m_1 = 0$ and $m_2 = 1$ occupied, i.e. $\Delta m = 1$ while all noncompact states have $\Delta m > 1$. This means that between 0 and 2π there will be one maximum for the ground state, the two electrons being at the opposite side of the ring. For the noncompact states there are two or more maxima between 0 and 2π and the wave functions will resemble excited states of a harmonic oscillator, i.e. vibrational states (actually in the two-electron case they are exactly those of a single particle in a 1D potential box).

Let us now generalize this analysis to a general case with N electrons. To this end we determine the square of the many-body wave function, $|\Psi(\{\varphi_i\})|^2$, in terms of the normal modes of classical harmonic vibrations. The equilibrium positions of classical particles are $\varphi_j^0 = 2\pi j/N$. The displaced positions of the particles corresponding to a normal mode ν are

$$\varphi_i^\nu = \varphi_i^0 + A \sin(\nu(i - \frac{1}{2})2\pi/N), \quad (10)$$

where ν is an integer ($1 \cdots N/2$) and A the amplitude of the oscillation.

Figure 3 shows $|\Psi(\{\varphi_i^\nu\})|^2$ for the different yrast states of a ring with 8 electrons, as a function of the amplitude A of the classical oscillation. In the case of a compact state (denoted by A in Fig. 1) $|\Psi|^2$ decreases rapidly with increasing A for all ν , as seen in the uppermost panel. This means that particles appear as being localized at the sites of classical particles with a repulsive interaction. For the non-compact yrast states (B and C in Fig. 1 and so on) the maximum of $|\Psi|^2$ is reached with a finite value of A so that $\nu = 1$ corresponds to state B, $\nu = 2$ corresponds to C, etc. The insets of the figure show the positions of the electrons at the maximum $|\Psi|^2$ of the corresponding figure. Clearly, there seems to be a correspondence between the different yrast states of *noninteracting spinless* electrons and vibrational modes of classical *interacting* particles in a ring.

The conclusion of this section is that the yrast spectrum of noninteracting spinless particles can be understood as rotational vibrational spectrum of classical particles with a repulsive interaction: The compact states

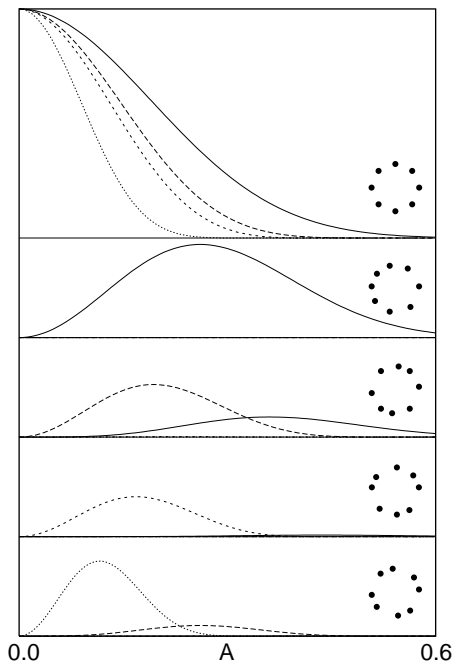


FIG. 3: The correlation of different quantum states of noninteracting electrons with the electron localization at the sites determined by the classical harmonic vibrational modes, as a function of the amplitude of the atomic displacement from the classical equilibrium position, i.e. $|\Psi(\{\varphi\})|^2$ as a function of A of Eq. (10). The panels from top to bottom correspond to quantum states $(\uparrow\uparrow\uparrow\uparrow\uparrow\uparrow\uparrow)$, $(\uparrow\uparrow\uparrow\uparrow\uparrow\uparrow \circ \uparrow)$, $(\uparrow\uparrow\uparrow\uparrow \circ \uparrow\uparrow)$, $(\uparrow\uparrow\uparrow\uparrow \circ \uparrow\uparrow)$, $(\uparrow\uparrow\uparrow \circ \uparrow\uparrow\uparrow)$, respectively, where \circ refers to an empty angular momentum state. The solid, long-dashed, short-dashed, and dotted lines correspond to $\nu = 1, 2, 3,$ and $4,$ respectively.

are purely rotational states, and the non-compact states correspond to vibrational excitations.

V. CLASSICAL INTERACTING ELECTRONS IN A STRICTLY 1D RING

A finite number of classical interacting particles in a strictly 1D ring will have discrete vibrational frequencies, which, after quantization, will give the quantum mechanical vibrational energies $\hbar\omega_\nu$. We assume a monotonic repulsive pairwise potential energy $V(r)$ between the particles, where r is the direct inter-particle distance. The potential energy can be written as

$$E = \frac{1}{2} \sum_{i \neq j}^N V \left(2R \left| \sin \left(\frac{\varphi_i - \varphi_j}{2} \right) \right| \right), \quad (11)$$

where R is the radius of the ring and φ_i the position (angle) of particle i . For any pair potential V it is straight-

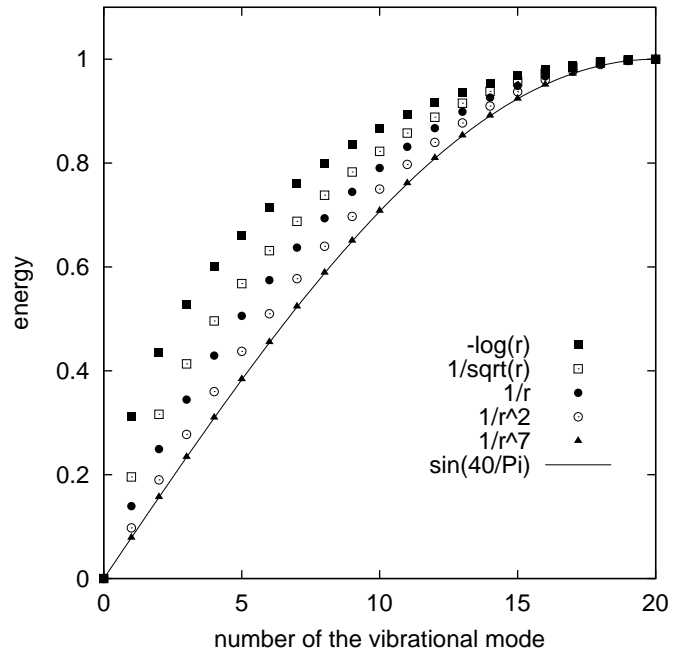


FIG. 4: Vibrational modes of 40 classical particles in a 1D ring. Different symbols correspond to different forms of the repulsive interaction between the particles, as indicated in the figure. The solid line is the result of a nearest neighbour harmonic model. The energies are scaled so that the highest vibrational energy for each potential is one.

forward to solve (numerically) the vibrational modes. In the case of a short range potential, reaching only to the nearest neighbours, one recovers the text-book example of acoustic modes of an infinite 1D lattice[45] (now only discrete wave vectors are allowed due to the finite length $2\pi R$)

$$\hbar\omega_\nu = C \sin \left(\frac{\nu\pi}{N} \right), \quad (12)$$

where C is a constant (proportional to the velocity of sound) and ν an integer.

Figure 4 shows the classical vibrational energies for different pair potentials $-\ln(r)$, $1/\sqrt{r}$, $1/r$, $1/r^2$, and $1/r^7$. Naturally, when the range of the potential gets shorter the vibrational energies approach that of the nearest neighbour interaction, Eq.(12), also shown. Note that the vibrational energies of the Coulomb interaction ($1/r$) do not differ markedly from those of $1/r^2$ -interaction. The latter has the special property that the energies agree exactly with the quantum mechanical energies of noninteracting spinless fermions, as discussed in section IX E.

In addition to the vibrational energy, the classical system can have rotational energy determined by the angular momentum: $E_{\text{rot}} = \frac{1}{2} NmR^2 \dot{\theta}^2$ (NmR^2 being the moment of inertia and $\dot{\theta}$ the angular velocity). Quantization of the vibrational and rotational energies gives the

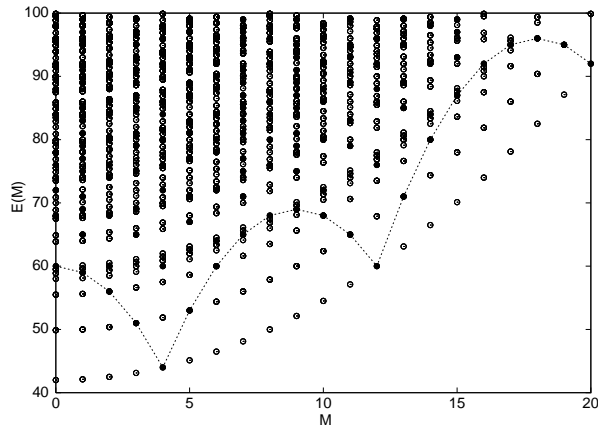


FIG. 5: Low-energy spectrum of eight electrons interacting with infinitely strong δ -function interaction. The black dots indicate the state with maximum spin ('spinless electrons'). White circles give the energies of other spin states. The spectrum is identical with the rotation-vibration spectrum of eight particles interacting with $1/r^2$ -interaction.

energy spectrum

$$E = E_{\text{rot}}(M) + E_{\text{vib}}(\{n_\nu\}) = \frac{\hbar^2 M^2}{2NmR^2} + \sum_\nu n_\nu \hbar \omega_\nu, \quad (13)$$

where M is the (total) angular momentum and n_ν the number of phonons ν .

Figure 5 shows the rotational vibrational spectrum derived from Eq.(13) for eight particles with $1/r^2$ interaction. It agrees exactly with that calculated quantum mechanically for electrons with (an infinite) δ -function interaction (see Section IX). It is important to notice that since the vibrational states are fairly independent of the interparticle interaction, the quantum mechanical spectrum close to the yrast line is expected to be qualitatively the same irrespective of the interaction.

Quantum mechanics plays an important role, however, when the Pauli exclusion principle is considered. The requirement of the antisymmetry of the total wave function restricts what spin-assignments can be combined with a certain rotation-vibration state. For example, for a completely polarized ring (maximum spin) only certain rotational vibrational states are allowed, as shown in Fig. 5. Group theory can be used to analyze the possible spin-assignments[46, 47] in a similar way as done in rotating molecules[48, 49].

In the case of bosons (with $S = 0$) the total wave function has to be symmetric, and the allowed rotation-vibration states are exactly the same as for spin-1/2-particles in the fully polarized state. Figure 5 is then also a 'general' result for eight bosons in a quantum ring (assuming the interaction to be repulsive).

VI. EFFECT OF A MAGNETIC FLUX – PERSISTENT CURRENTS

We consider a magnetic flux going through the quantum ring in such a way that the magnetic field is zero at the radius of the ring. This can be modelled, for example, by choosing the vector potential to be (in circular cylindrical coordinates)

$$A_r = A_z = 0, \quad A_\varphi = \begin{cases} \frac{B_0 r}{2}, & \text{if } r \leq r_c \\ \frac{B_0 r_c^2}{2r} = \frac{\Phi}{2\pi r}, & \text{if } r > r_c \end{cases} \quad (14)$$

which gives a flux $\Phi = \pi r_c^2 B_0$ penetrating the ring in such a way that the field is constant inside r_c and zero outside. If the ring is in the field-free region ($R > r_c$) the electron states depend only on the total flux penetrating the ring.

The solutions of the single particle Schrödinger equation of an infinitely narrow ring ,

$$\frac{1}{2m_e} \left(-\frac{i\hbar}{R} \frac{\partial}{\partial \varphi} - \frac{e\Phi}{2\pi R} \right)^2 \psi(\varphi) = \epsilon \psi(\varphi), \quad (15)$$

can be still written as flux-independent plane waves $\psi_m = \exp(im\varphi)$, but the corresponding single particle energies now depend on the flux as

$$\epsilon(m, \Phi) = \frac{\hbar^2}{2m_e R^2} \left(m - \frac{\Phi}{\Phi_0} \right)^2. \quad (16)$$

The many-body wave function is still the same Slater determinant as without the field, while the total energy becomes

$$E(M, \Phi) = E(M, 0) - \frac{\hbar^2 M}{m_e R^2} \left(\frac{\Phi}{\Phi_0} \right) + \frac{\hbar^2 N}{2m_e R^2} \left(\frac{\Phi}{\Phi_0} \right)^2 \quad (17)$$

The effect of increasing flux is not to change the level structure but to tilt the spectrum, say of Fig. 2, such that the global minimum of the total energy jumps from one compact state to the next compact state. Note that Eq.(17) is true also for interacting electrons in a strictly one-dimensional ring. This follows from the fact that any good angular momentum state can be written as a linear combination of Slater determinants of non-interacting states. For each of these, the last two terms are the same, while $E(M, 0)$ depends on the interactions.

Alternatively, one may perform a unitary transformation to obtain a description of the system in terms of a *field-free* Hamiltonian, but with multivalued wavefunctions ("twisted boundary conditions"). Let us choose a gauge $\mathbf{A} = \nabla \chi$ (which ensures that $\mathbf{B} = \nabla \times \mathbf{A}$ is zero at the ring; in a strictly one-dimensional ring one may write $\chi(\varphi) = \Phi \varphi / (2\pi)$) and consider the unitary transformation

$$\psi \rightarrow \psi' = U \psi \quad (18)$$

$$H \rightarrow H' = U H U^{-1} \quad (19)$$

where the operator U is defined as

$$U = e^{-ie/\hbar \int \mathbf{A} \cdot d\mathbf{l}} = e^{-ie/\hbar \chi}. \quad (20)$$

Obviously, the eigenspectrum will be conserved under this transformation – if $H\psi = E\psi$, then $H'\psi' = UHU^{-1}U\psi = UH\psi = E\psi'$. It is easy to show that the effect of this transformation on the Hamiltonian is to cancel out the gauge field, i.e.

$$U\left(\frac{-i\hbar}{R} \frac{\partial}{\partial \varphi}\right)U^{-1} = \frac{-i\hbar}{R} \frac{\partial}{\partial \varphi} + eA_\varphi, \quad (21)$$

and the Hamiltonian takes the field-free form

$$H' = -\frac{\hbar^2}{2m_e R^2} \frac{\partial^2}{\partial \varphi^2}. \quad (22)$$

Meanwhile, the wave function now picks up a phase $(-ie/\hbar)\chi$ when moving along a given path, even though it moves in a region where the magnetic field is zero. This is the so-called Aharonov-Bohm effect[1]. In particular, if an electron moves along a closed path around the flux tube, the Aharonov-Bohm phase becomes

$$\frac{-ie}{\hbar} \Delta\chi = \oint_{2\pi R} \nabla\chi \cdot d\mathbf{l} = \frac{-ie}{\hbar} \oint_{2\pi R} \mathbf{A} \cdot d\mathbf{l} = \frac{-ie}{\hbar} \int_{\pi R^2} \mathbf{B} \cdot d\mathbf{s} = \frac{-ie}{\hbar} \Phi. \quad (23)$$

In other words, the boundary condition has now changed. While the original wave function satisfies periodic boundary conditions, $\psi(\varphi) = \psi(\varphi + 2\pi)$, for the new wave function we have the condition $\psi'(\varphi + 2\pi) = \psi'(\varphi) \exp(-ie\Phi/\hbar)$, i.e. “twisted boundary conditions”. Note that this boundary condition naturally leads to periodic eigenvalues $\epsilon'(m') = \epsilon'(m' + \Phi/\Phi_0)$, in the same way as the Bloch condition for electron states in a periodic lattice leads to the periodicity of the eigenenergies in the reciprocal lattice[45].

The spectrum (16) is clearly periodic in flux with period Φ_0 . Any *given* eigenstate $\psi'_m = \exp(i(m - \Phi/\Phi_0)\varphi)$, however, will have its angular momentum eigenvalue shifted by one as the flux is changed by one flux quantum.

The persistent current of a quantum ring can be written in general as

$$I(\Phi) = -\frac{\partial F}{\partial \Phi}, \quad (24)$$

where F is the free energy of system. To illustrate this

in the simplest possible case, consider the Schrödinger equation for a one-electron ring,

$$-\frac{\hbar^2}{2m} D^2 \psi_m(\varphi) = E_m \psi_m(\varphi) \quad (25)$$

where

$$D = \frac{1}{R} \frac{\partial}{\partial \varphi} - \frac{ie}{\hbar} A_\varphi. \quad (26)$$

Multiplying both sides of Eq.(25) by ψ_m^* from the left and integrating along the circumference of the ring one gets

$$E_m = -\frac{1}{2m_e} \int_0^{2\pi} R d\varphi \psi_m^*(\varphi) D^2 \psi_m(\varphi). \quad (27)$$

Using the expression (14) for the gauge field and taking the derivative with respect to flux one obtains, after an integration by parts,

$$\frac{\partial E_m}{\partial \Phi} = \frac{1}{2\pi R} \frac{ie\hbar}{2m_e} \int_0^{2\pi} R d\varphi [\psi_m^* D \psi_m - \psi_m D^* \psi_m^*] = -\frac{1}{2\pi} \int_0^{2\pi} d\varphi j(\varphi) \equiv -I_m, \quad (28)$$

where we have identified the RHS with the 1D current (density) associated with the state m . (Note that $j(\varphi)$ has to be independent of the angle φ). Obviously, the same argument applies for a non-interacting many-body system where the contributions from different angular momentum states are simply summed. The same is true in the presence of interactions due to the fact that all flux dependence is in the kinetic energy term of the many-body Hamiltonian (see discussion after Eq.(17)).

Due to the periodicity of the energy spectrum, the persistent current will be a periodic function of the flux. In the case of noninteracting spinless electrons, the period is Φ_0 , owing to the fact that the minimum energy for any flux corresponds to a compact state. As will be seen in Sec. XII, the electron-electron interactions can change the periodicity to $\Phi_0/2$ or to Φ_0/N .

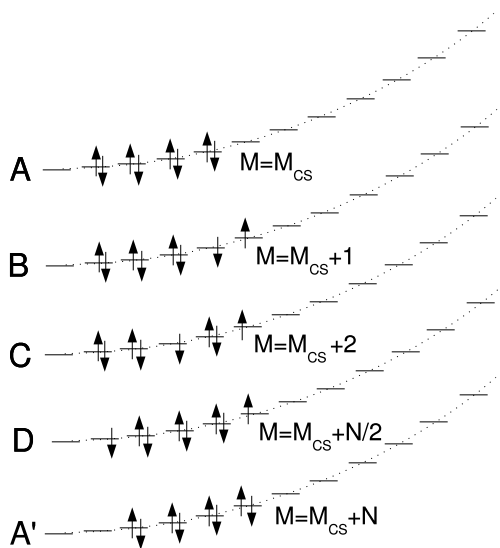


FIG. 6: Configurations of the many-body states of eight noninteracting electrons with spin in a ring. A, A', and D give local minima in the yrast line, while B and C correspond to 'vibrational excitations'.

VII. NONINTERACTING PARTICLES WITH SPIN

The spin degree of freedom allows two electrons for each single particle orbital. The yrast states of the many-body spectrum are still consisting of compact or nearly compact states, but now for each spin component as shown in Fig. 6. The corresponding yrast spectrum for 8 electrons is shown in Fig. 2 in comparison to the spectrum of spinless electrons. The total spin of the states A (in Fig. 6) is $S = 0$ while for all other states have either $S = 0$ (singlet) or $S = 1$ (triplet) as can easily be deduced from Fig. 6 by considering the possible ways to arrange the S_z -components in the orbitals with only one electron.

The yrast spectrum now consists of downward cusps at angular momenta $M = nN/2$, but those minima corresponding to $S = 0$ compact states are deeper. In the case of noninteracting electrons with spin there is not such a clear relation to classical rotation-vibration spectrum as in the case of spinless noninteracting case discussed above. One could consider spin-up and spin-down states separately as spinless systems which do not interact with each other. However, considering the complete many-body spectrum one should notice that the energy of state B in Fig. 6 is degenerate with the state where the spin-up system has five electrons and the spin-down system only three.

The persistent current of the noninteracting system with the spin is again a periodic function of the flux. The period is Φ_0 like in the case of spinless electrons.

When the field is increased, the ground state shifts from a compact state (of the kind A in Fig. 6) to the next similar state A', i.e. the angular momentum shifts with N . At the transition point the three levels, A, D and A', are actually degenerate, but the D-states do not change the periodicity of the persistent current. However, the amplitude of the persistent current is only half of that of the spinless electrons.

So far we have considered only even numbers of electrons. In the case of an odd number of electrons, the spinless case is very similar to that of even numbers, the only difference being a phase shift of $\Phi_0/2$ of the periodic oscillations. However, in the case of electrons with spin, the odd number of electrons has an effect also on the amplitude of the persistent current: For a large number of electrons the amplitude for odd numbers of electrons is exactly twice that of even numbers of electrons, as first shown by Loss and Goldbart[50]. This effect is sometimes referred to as a parity effect.

VIII. NONINTERACTING ELECTRONS IN A LATTICE

Instead of a continuum ring, we will now consider noninteracting electrons in a strictly 1D ring with a strong periodic potential. In this case the standard solid state physics approach is the tight-binding model where the Hamiltonian matrix can be written as

$$H_{ij} = \begin{cases} \epsilon_0 & \text{if } j = i \\ -t & \text{if } j = i \pm 1, \end{cases} \quad (29)$$

where the diagonal terms describe the energy level at a lattice site and the off-diagonal terms describe the hopping between the levels. This simplest tight-binding model assumes one bound state per lattice site and is often called the Hückel model or CNDO-model (complete neglect of differential overlap).

Assuming the ring, with radius R , to have L lattice sites, the problem of solving the eigenvalues becomes a text-book example of 1D band structure[45], and the single electron eigenvalues can be written as

$$\epsilon(k) = \epsilon_0 - 2t \cos(ka) = \epsilon_0 - 2t \cos\left(\frac{2\pi}{L}m\right), \quad (30)$$

where a is the lattice constant, k the wave vector and m an integer. The last step follows from the facts that the lattice constant is $a = 2\pi R/L$, and in a finite ring k will have only discrete values $k = m/R$. Notice that in the large L limit, $m/L \rightarrow 0$, the energy spectrum is equivalent with that of free electrons, Eq. (2), if we choose the tight-binding parameters as $\epsilon_0 = 2t$ and $t = \hbar^2/2m_e a^2$. In this case the quantum number m gets the meaning of the orbital angular momentum. (This equivalence of the tight-binding model and free electron model is valid for simple lattices of any dimension and can be derived also

by discretizing the Laplace operator of the free particle Schrödinger equation[51]).

The many-body state is again a simple Slater determinant of the single particle states with the total energy

$$E = N\epsilon_0 - 2t \sum_{j=1}^N \cos\left(\frac{2\pi}{L}m_j\right), \quad (31)$$

where the selection of the 'angular momenta' m_j is restricted by the Pauli exclusion principle. For example, in the polarized case (spinless electrons) all m_j must be different, and the ground state is obtained with a compact state where the m_j 's are consecutive integers as in the case of free electrons. Similarly, we can identify 'vibrational states' by making a hole in the compact state as will be demonstrated in more detail in the following sections.

IX. INTERACTING ELECTRONS ON A LATTICE: THE HUBBARD MODEL

A. Model and exact diagonalization

A much studied approach to quantum rings and persistent currents is the Hubbard model[52, 53, 54, 55, 56,

$$H = -t \sum_{i=1}^N \sum_{\sigma} \left(e^{-i2\pi\phi/L} c_{i+1,\sigma}^{\dagger} c_{i,\sigma} + e^{i2\pi\phi/L} c_{i,\sigma}^{\dagger} c_{i+1,\sigma} \right) + U \sum_{i=1}^N \hat{n}_{i\uparrow} \hat{n}_{i\downarrow}. \quad (32)$$

Here, the operator $c_{i,\sigma}^{\dagger}$ ($c_{i,\sigma}$) creates (annihilates) an electron with spin σ at site i ; $\hat{n}_{i\sigma} = c_{i,\sigma}^{\dagger} c_{i,\sigma}$ is the number operator for spin- σ electrons at site i . The first part of (32) describes the hopping of electrons between neighbouring sites ("kinetic term") while the last part gives the repulsion between electrons occupying the same site. We will set the hopping parameter $t = 1$ for simplicity.

For small numbers of electrons N and lattice sites L the Hubbard Hamiltonian can be solved exactly by diagonalization of the Hamiltonian matrix. We use an occupation number basis (see e.g. [61]) $|\Psi_{\alpha}\rangle = |n_{\alpha 1\uparrow}, n_{\alpha 2\uparrow} \dots n_{\alpha L\uparrow}; n_{\alpha 1\downarrow} \dots n_{\alpha L\downarrow}\rangle$ where the z -component of the total spin is fixed, i.e. $\sum_i n_{\alpha i\uparrow} = N_{\uparrow}$ and $\sum_i n_{\alpha i\downarrow} = N_{\downarrow}$ ($N = N_{\uparrow} + N_{\downarrow}$). Taking matrix elements $\langle\Psi_{\alpha}|H|\Psi_{\alpha'}\rangle$ gives us a matrix with dimension $\binom{L}{N_{\uparrow}}\binom{L}{N_{\downarrow}}$. The eigenvalues of this matrix are the exact many-body energy levels of the Hubbard Hamiltonian. For a given total spin S , the energy eigenvalues do not depend on S_z (there is no Zeeman splitting since we assume the magnetic field to be nonzero only inside the ring). In the case of an even N we can choose $S_z = 0$, or

57, 58, 59]. It describes electrons on a discrete lattice with the freedom to hop between lattice sites, and the Coulomb interaction is represented by an on-site repulsion. An interesting feature of the Hubbard ring is that, despite being a strongly correlated electron system, it can be solved exactly. For a small number of particles the solution can be found by direct diagonalization of the Hamiltonian matrix as discussed first. For any number of particles another solution technique, the Bethe ansatz, can be used. This technique is most suitable in the limit of infinite U (so-called t -model) and will be addressed in the next subsection. The Hamiltonian describing the Hubbard model for an N -electron ring with L lattice sites, in the presence of a magnetic flux $\phi = \Phi/\Phi_0$ piercing the ring, can be derived with the help of the unitary transformation introduced in Sec.VI (the flux dependence was first derived by Peierls[60]):

$N_{\uparrow} = N_{\downarrow} = N/2$, and the diagonalization of the Hamiltonian will give us all possible eigenvalues (for odd N we take $S_z = 1/2$). The easiest way to solve the *total* spin of a given energy state is then to repeat the computation with all possible values of S_z and look at the degeneracies. (Note that the matrix dimension is largest for $S_z = 0$ and thus solving the matrix for all $S_z > 0$ takes less computation than solving the $S_z = 0$ case).

B. The t -model

In the following we will first focus on the strong repulsion limit $U \rightarrow \infty$, which was first discussed nearly 20 years ago[62]; we shall return to finite U effects later. In this limit, the system is equivalently described by the simpler " t -model" Hamiltonian[63, 64]

$$H_t = PH_{kin}P, \quad (33)$$

where H_{kin} is the kinetic (hopping) term of (32) and P denotes a projection operator which eliminates all states

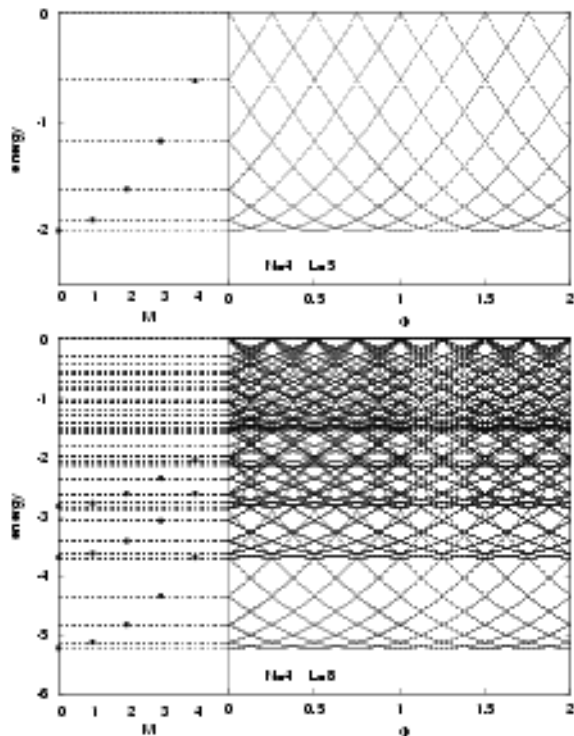


FIG. 7: Energy spectra of rings of four electrons in five (upper panel) and eight (lower panel) sites, calculated with the t -model Hamiltonian. The right hand side shows the energy levels as a function of the flux (in units of Φ_0). On the left, the zero flux energy levels are shown as a function of the angular momentum M (black dots). Note that the $L = 8$ case shows several vibrational bands. Only negative energy levels are shown since the spectrum is symmetric around zero energy.

with doubly occupied sites. It can be shown [63] that this projected Hamiltonian is equivalent to a tight-binding Hamiltonian describing *spinless fermions*. Moreover, going to large but *finite* U , near half filling, the Hubbard model reduces to the so-called $t - J$ model, i.e. the t -model (33) plus a Heisenberg term $J \sum_i \mathbf{S}_i \cdot \mathbf{S}_{i+1}$ [64]. In other words the translational and spin degrees of freedom get decoupled. We will return to the $t - J$ model in Sec. IX F.

In the next subsection we will describe how solutions of the t -model can be constructed using the Bethe ansatz. However, for a small number of electrons and lattice sites (N and L) the direct diagonalization has the advantage of giving all the eigenvalues at once and some information of the many-body state is more transparent. The results shown for small discrete rings are obtained either with diagonalization techniques or using the Bethe ansatz solution. It should be stressed that both methods are exact and give the same results.

We will first study four electrons (with spin) in a lattice having at least one empty site. Figure 7 shows the energy spectrum for $L = 5$ and 8. The right-hand panels

show the energies as a function of the magnetic flux piercing the ring, while the left-hand side shows the lowest energies at zero flux, analyzed with respect to the total angular momentum, for the different “vibrational bands” in the spectra. The following general features should be noted: The energy (and thus the persistent current) has a periodicity Φ_0/N . In particular, as first discussed by Kusmartsev[54] and by Yu and Fowler[55], in the ground state there are N cusps in every flux period; increasing the flux makes the ground state jump from one angular momentum state to the next. (A more general discussion of the periodicity of the ground state will be given in section XII.) Each *individual* state, on the other hand, is a harmonic (cosine) function of the flux, with periodicity $L\Phi_0$, in accordance with the periodicity of the Hamiltonian. Thus, the energy of each individual state has the form, up to an overall phase shift,

$$E \sim \cos \left[\frac{2\pi}{L} \left(-\frac{\Phi}{\Phi_0} - \frac{p}{N} \right) \right] \quad (34)$$

with p an integer. Obviously, the (kinetic) energy collapses to zero in the case of half filling, $L = N$, as in this case there is no freedom to hop. Surprisingly, however, the above generic flux dependence of the lowest states of the spectra is obtained even for a single free site (i.e. $L = 5$ for $N = 4$). For $L > N + 1$, there are several “energy bands” consisting of states with different amplitude; the number of bands increases with the number of empty sites. As will be discussed below (Sec. IX D), the lowest energy state at any given flux corresponds to the rotational band without vibrational energy, while the higher bands can be interpreted as the vibrational states of the system.

It should be noted that each individual energy level in Fig. 7 still has a spin degeneracy: Two or more states with different *total* spin S belong to each energy level. The magnetic field can not separate these since we have neglected the possible Zeeman splitting. A finite U will separate the states belonging to different total spin as will be shown in Sec. IX F, but will still leave the degeneracy due to the S_z .

C. Bethe ansatz

The Hubbard model in 1D can in fact be solved exactly, in terms of the Bethe ansatz, as shown by Lieb and Wu in 1968[11]. The corresponding solution for a Hubbard ring in the presence of an Aharonov-Bohm flux has later been discussed by a number of authors [54, 55, 57, 65, 66]. Bethe ansatz solutions can be used to construct not only the ground state but in fact the entire spectrum presented in the previous section. According to this method, the energy of a given many-body state may be written as

$$E = -2 \sum_{j=1}^N \cos k_j \quad (35)$$

where the numbers k_j can be found by solving the set of Bethe equations

$$Lk_j = 2\pi I_j - \Phi - \sum_{\beta=1}^{N_\uparrow} 2 \tan^{-1}[4(\sin k_j - \lambda_\beta)/U] \quad (36)$$

$$\sum_{j=1}^N 2 \tan^{-1}[4(\lambda_\alpha - \sin k_j)/U] = 2\pi J_\alpha + \sum_{\beta=1}^{N_\uparrow} 2 \tan^{-1}[2(\lambda_\alpha - \lambda_\beta)/U]. \quad (37)$$

For obtaining the whole energy spectrum, the unknown (complex) constants k_j and λ_β have to be solved for different quantum numbers I_j and J_α , which are restricted to be integers or half-integers depending on the numbers N and N_\uparrow . For example, if N and N_\uparrow both are even, I_j must be an integer and J_j a half-integer. The total (canonical) angular momentum corresponding to the quantum numbers is given by

$$M = \sum_{j=1}^N I_j + \sum_{\alpha=1}^{N_\uparrow} J_\alpha. \quad (38)$$

In the general case of a finite U the nonlinear Bethe equations turn out to be difficult to solve numerically, at least for some quantum numbers[67]. For small systems (N and L small) it is easier to find *all* eigenvalues by a direct diagonalization of the Hamiltonian matrix as explained in the previous section.

In the limit of infinite U , however, the Bethe ansatz solution becomes particularly simple. In this case the quantum numbers $k_j \in [0, 2\pi)$ are simply given by[54, 55]

$$k_j = \frac{2\pi}{L} \left[I_j - \frac{p}{N} + -\frac{\Phi}{\Phi_0} \right] \quad (39)$$

with

$$p = - \sum_{\alpha=1}^{N_\uparrow} J_\alpha. \quad (40)$$

So a given solution is constructed for a fixed N_\uparrow , i.e. a fixed value of the z -component of the spin. The quantum numbers I_j and J_α are related to the charge- and spin degrees of freedom, respectively. In the case we shall

consider, even N , the I_j :s are integers (half-odd integers) and the J_α :s are half-odd integers (integers) if N_\uparrow is even (odd). In practice, all eigenvalues can be found by letting p run over all integers and choosing all possible sets of I_j :s with the restriction $I_{max} - I_{min} < L$.

Ground state of the t -model

In analogy to the non-interacting case, the states forming the outermost band (see Fig. 7), i.e. states which become the ground state at some value of the flux, are compact states in the quantum numbers $\{I_j\}$. At zero flux, these are of course just the yrast states (see left-hand panels in Fig. 7). For example, if N and M are both even, the quantum numbers $\{I_j\}$ are consecutive integers, $I_j = -N/2, -N/2 + 1, \dots, N/2 - 1$. The corresponding total energy, Eq.(35), as function of flux, becomes[55]

$$E_0 = -E_m \cos \left[\frac{2\pi}{L} \left(-\frac{\Phi}{\Phi_0} - \frac{p}{N} + D_c \right) \right], \quad (41)$$

where $D_c = (I_{max} + I_{min})/2$ and

$$E_m = 2 \frac{\sin(N\pi/L)}{\sin(\pi/L)}. \quad (42)$$

The integer p should be chosen, for given flux, such as to minimize the energy. Of course, there are in general several ways of choosing the ‘‘spin quantum numbers’’ J_α to give the same sum, leading to a large degeneracy of the state. This has to do with the fact that spin excitations are massless in the limit of the t -model; for finite U this degeneracy would be lifted. Note that the energy collapses to zero for half filling, i.e. when $L = N$.

As a simple illustration, consider the example $N = 4$ at zero flux. Then, $I_j = -2, -1, 0, 1$, $D_c = -1/2$ and

$$\sum_j \cos k_j = \cos \left[\frac{2\pi}{L} \left(-\frac{p}{N} - \frac{1}{2} - \frac{3}{2} \right) \right] + \cos \left[\frac{2\pi}{L} \left(-\frac{p}{N} - \frac{1}{2} - \frac{1}{2} \right) \right] \quad (43)$$

$$+ \cos \left[\frac{2\pi}{L} \left(-\frac{p}{N} - \frac{1}{2} + \frac{1}{2} \right) \right] + \cos \left[\frac{2\pi}{L} \left(-\frac{p}{N} - \frac{1}{2} + \frac{3}{2} \right) \right] \quad (44)$$

$$= 2 \left(\cos \frac{\pi}{L} + \cos \frac{3\pi}{L} \right) \cos \left[\frac{2\pi}{L} \left(\frac{p}{N} + \frac{1}{2} \right) \right] \quad (45)$$

$$= \frac{\sin(4\pi/L)}{\sin(\pi/L)} \cos \left[\frac{2\pi}{L} \left(\frac{p}{N} + \frac{1}{2} \right) \right]. \quad (46)$$

It is easy to check that the “amplitudes”, $-2\sin(4\pi/L)/\sin(\pi/L)$ agree with those in Fig. 7 for $L = 5$ and 8 . Note that the choice of the “central value” D_c as an overall phase shift makes the sum symmetric; one obtains *pairs*, $\cos \left[\frac{2\pi}{L} (-p/N + D_c \pm \gamma) \right]$, so that, when writing out the sum, all $\sin(2\pi\gamma/L)$ -terms cancel. This also implies that shifting all the I_j :s by the same amount, does not alter the total energy (41); it only changes the overall phase shift D_c . The integer p is related to the angular momentum M , see Eq.(38). This construction gives not only the ground state but, for fixed flux, all energy levels of the lowest band, corresponding to different p .

Higher bands

Generally, excitations can be constructed within the Bethe ansatz by introducing *holes* in the ground state dis-

tribution of the quantum numbers I_j and J_α [66]. Naturally, these states are related to the “non-compact” states of noninteracting fermions in a strictly 1D ring, discussed in Sec. III. The higher bands in our spectra correspond to charge excitations, i.e. holes in the I_j (J_α -excitations do not cost any energy in the infinite U limit), and this reproduces exactly all the energies obtained numerically in the previous section. We will illustrate this procedure with a few examples for $N = 4$, $M = 2$. The lowest possible “excitation” in the charge quantum numbers I_j is lifting the topmost one by one step,

$$\{I_j\} = -2, -1, 0, 2, \quad (47)$$

and the corresponding k_j as given in Eq.(39). The resulting energy is

$$E_1 = -2 \sum_j \cos k_j \quad (48)$$

$$= -2 \left(1 + 2 \cos \frac{4\pi}{L} + \cos \frac{2\pi}{L} \right) \cos \left[\frac{2\pi}{L} \left(-\frac{p}{N} - \frac{\Phi}{\Phi_0} \right) \right] - 2 \sin \frac{2\pi}{L} \sin \left[\frac{2\pi}{L} \left(-\frac{p}{N} + \frac{\Phi}{\Phi_0} \right) \right]. \quad (49)$$

This again gives a band of states which are cosine functions of the flux, with period $L\Phi_0$. Differentiating E_1 wrt. $\alpha \equiv \frac{2\pi}{L} \left(-\frac{p}{N} - \frac{\Phi}{\Phi_0} \right)$, one finds the “amplitude” of this band as

$$E_{1,min} = -2 \left(1 + 2 \cos \frac{4\pi}{L} + \cos \frac{2\pi}{L} \right) \cos \alpha_{min} - 2 \sin \frac{2\pi}{L} \sin \alpha_{min} \quad (50)$$

with

$$\alpha_{min} = \tan^{-1} \left[\frac{\sin \frac{2\pi}{L}}{1 + 2 \cos \frac{4\pi}{L} + \cos \frac{2\pi}{L}} \right]. \quad (51)$$

Note that at *zero* flux, the lowest state of this band may have an energy *larger* than $E_{1,min}$ – the nearest minimum may occur at a finite flux. This is because p has to be an integer, and $(LN/2\pi)\alpha_{min}$ is not generally an integer (except for some special values of L).

The simplest example for four particles is $L = 6$. In this case $\alpha_{min} = \pi/3$, i.e. the energy of the state (47) has a minimum at zero flux with $p/N = -1$ and $E_{1,min} = -\cos(\pi/3) - \sqrt{3}\sin(\pi/3) = -2$.

This method is easily generalized to construct higher bands. For example, the second excitation band corresponds to, for four particles, $\{I_j\} = -2, -1, 1, 2$ with

TABLE I: Total weight of the most important configurations of the many-body states of different vibrational states for the t -model ring with $L = 8$ and $N = 4$. The configuration is shown as filled and empty circles indicating whether or not there is an electron in the corresponding site. The second column shows the number of such states (not including the degeneracy coming from the spin configuration). The last three columns show the total weights of these states for the vibrational ground state (w_0) and the two vibrational bands. The total weights are the same for all rotational states and different spin states belonging to the same vibrational mode.

configuration	n	w_0	w_1	w_2
○ ● ○ ● ○ ● ○ ●	8	0.1248	0.0000	0.0000
○ ● ○ ● ● ○ ● ○	32	0.1824	0.2136	0.0624
○ ● ● ○ ○ ● ● ○	16	0.0624	0.0000	0.1256

energy

$$E_2 = -4 \left(\cos \frac{2\pi}{L} + \cos \frac{4\pi}{L} \right) \cos \left[\frac{2\pi}{L} \left(\frac{p}{N} + \frac{\Phi}{\Phi_0} \right) \right]. \quad (52)$$

The higher (inner) bands constructed in this way may be interpreted as corresponding to vibrational excitations. As an example, we have examined, for the $N = 4$, $L = 8$ solutions of the t -model, which electron-hole configurations have the largest amplitude (in the many-body wavefunction) in each of the three lowest bands. Table I shows the weights of the most important basis states for the ground state and for the two lowest vibrational states. These are consistent with the classical motion of electrons in the first vibrational modes.

D. Vibrational bands

In the limit $L \rightarrow \infty$, i.e. infinitely many sites, the t -model is expected to correspond to a system of non-interacting (spinless) particles in the continuum (as they no longer “see” the delta function interaction), in a similar way as the simple tight-binding model approaches to the continuum model when the number of lattice sites increases (see Sec. VIII). One way of illustrating that this is indeed the case, is to examine the ratios

$$R_n \equiv \frac{E_n - E_0}{E_1 - E_0}, \quad (53)$$

where E_i is the (minimum) energy of the i th excited band. In the case of non-interacting, spinless particles the energy, in units of $\hbar^2/(2m_e R^2)$, of an N -particle state at flux $\phi = \Phi/\Phi_0$ is given by

$$E = \sum_{i=1}^N (m_i - \phi)^2 \quad (54)$$

where m_i are the single particle angular momenta and the total angular momentum is $M = \sum m_i$. The minimum in energy of this state occurs at $\phi = M/N$ and is

given by $E_{min} = \sum_{i=1}^N m_i^2 - M^2/N$. As discussed in Sec. III, the ground state corresponds to filling consecutive angular momentum states, e.g. $m_i = 0, 1, \dots, N-1$. A set of $N/2$ excited states is constructed by creating 1-hole excitations, the lowest one being $m_i = 0, 1, \dots, N-2, N$. (Note that an overall shift of all the angular momenta does not change the minimum energy – it just occurs at a different flux.) Computing the ratios R_n as defined in Eq.(53) one finds

$$R_n \equiv \frac{n(N-n)}{N-1}. \quad (55)$$

As we shall see, these one-hole excitations in a sense correspond to fundamental phonon excitations. Moreover, it is easy to show that 2-hole excitations lead to ratios (in the limit $N \rightarrow \infty$) which are twice those in Eq.(55), thus corresponding to two-phonon excitations, etc.

Now, the same ratios can be recovered from the Bethe ansatz solution of the t -model, as given by equations (35) and (39): Constructing the set of excitations which correspond to one hole in the quantum numbers I_j , minimizing the energy as described in the previous section, and taking the limit $L \rightarrow \infty$, one again gets Eq.(55). This shows that the energy bands of the Hubbard model reduce to those of non-interacting particles in the limit of infinite repulsion and infinite number of sites. (Of course the correspondence between the t -model and free particles can also be seen using a similar argument as in section VIII: For the maximum spin state, $-p = \sum J_\alpha = 0$ in Eq.(38) so that the integers I_j correspond just to the single particle angular momenta.)

E. $1/d_{ij}^2$ interactions:

There is another type of interaction in one dimension which leads to the same set of excitation bands as above, namely $V_{ij} = 1/d_{ij}^2$, where d_{ij} is the distance between particles i and j . Models in 1D with this type of interaction are known as the Calogero- (on a line) or Sutherland model (on a circle) [43, 44] and have been studied extensively over the past three decades. What makes the Calogero (or Sutherland) model special, is that it mimics as closely as possible a system of free particles. Consider the N -particle Sutherland Hamiltonian,

$$H_S = - \sum_{i=1}^N \frac{\partial^2}{\partial x_i^2} + 2\lambda(\lambda-1) \sum_{i<j} \frac{1}{\left(2 \sin \left(\frac{x_i - x_j}{2}\right)\right)^2}, \quad (56)$$

where we have set the radius of the circle to 1. The complete excitation spectrum of this model can be found exactly in terms of the asymptotic Bethe ansatz (see e.g. [68] and references therein) and is remarkably simple. The total energy and angular momentum of a given state can be written as $E = \sum_j p_j^2$ and $P = \sum_j p_j$, respectively, where the quasi-momenta p_n are related to the

free angular momenta m_j by

$$p_j = m_j + \gamma \left(j - \frac{N+1}{2} \right), \quad (57)$$

where $\gamma = (\lambda - 4)/4$. In other words, the energy and total angular momentum take the same form as in the non-interacting case, with the interactions absorbed in the shift of the quasi-momenta. For each non-interacting many-body state characterized by a set of fermionic quantum numbers $\{m_j\}$ there is a corresponding state with quantum numbers $\{p_j\}$. Note that $P = \sum_j p_j = \sum_j m_j = M$. Now consider the Sutherland model in the presence of an Aharonov-Bohm flux piercing the ring. The energy of a given state can then be written as

$$E = \sum_j (p_j - \phi)^2 \quad (58)$$

and, as in the non-interacting case, is minimized for $\phi = M/N$,

$$E_{min} = \sum_j p_j^2 - M^2/N. \quad (59)$$

We want to compute the shift in energy of a many-body state as compared to the non-interacting one, which then will be used to compute the ratios R_n . Inserting the solution (57) into Eq.(58) one finds, up to an overall constant,

$$\Delta E(\gamma) = E_{min}(\gamma) - E_{min}(\gamma = 0) \quad (60)$$

$$= \gamma \left(\sum_{j=1}^N j m_j - (N+1)M \right). \quad (61)$$

Again constructing the set of one-hole excitations (in m_j) as before, one easily finds the *difference* between the shift of the n th excitation and the shift in the ground state,

$$\Delta E^{(n)}(\gamma) - \Delta E^{(0)}(\gamma) = \gamma (n(N-n)). \quad (62)$$

From this it immediately follows that the ratios R_n for the Sutherland model are the same as in the non-interacting case, see Eq.(55). In addition, recall section V where we performed a calculation of the normal modes for a set of *classical* particles on a ring with $1/d^2$ repulsion. In a semiclassical picture, the corresponding frequencies ω_j were then interpreted as the eigenfrequencies of the many-body problem, with energies $\hbar\omega_j$. Using these to compute the ratios R_n , one again obtains the same expression as above. This illustrates that the “single-particle excitations”, both in the non-interacting case and in the Sutherland model, can indeed be interpreted as corresponding to vibrational modes. (Cfr. the discussion of the free particle case in Sec. IV.)

F. Finite U

The Hubbard model with finite U can still be solved with the Bethe ansatz but now it requires numerical solution of the set of nonlinear equations (36). In the case

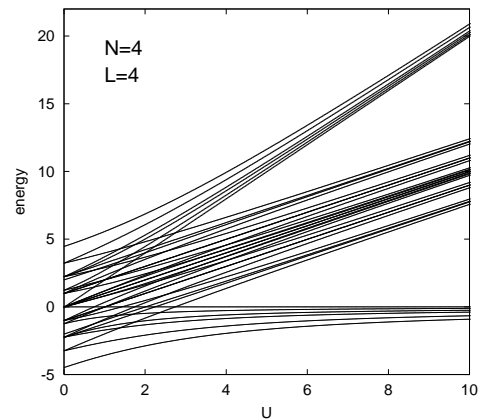


FIG. 8: Energy levels as a function of U for a four electron Hubbard ring with four sites.

of small number of electrons and sites a direct numerical diagonalization of the Hubbard Hamiltonian, Eq. (32), is in fact easier. The results shown in this section have been computed with the direct numerical diagonalization. As an example case we use again the 4 electron ring.

Figure 8 shows the energy spectrum for four electrons in four sites as a function of on-site interaction U . The results start from the noninteracting case (with spin). Increasing U separates the spectrum into different groups. The lowest group corresponds to states where all the electrons are mainly at different lattice sites while the two higher bands correspond to states where one or two electrons are at the same site, respectively. This can be seen by looking at the structure of the many-body states or simply by noticing that the energy of the higher groups of levels increase as $E \approx U$ and $E \approx 2U$.

The high- U limit of the lowest group of states can be explained with the so-called tJ -model. In the limit of large U the half-filled Hubbard model can be approximated as (see [64] and references therein)

$$H_{tJ} = H_t + \frac{J}{2} \sum_{i \neq j}^N \left(\mathbf{S}_i \cdot \mathbf{S}_j - \frac{1}{4} \right), \quad (63)$$

where H_t denotes the Hamiltonian of the infinite U limit (t model), $J = 4t^2/U$ and \mathbf{S}_i is a spin operator ($S = 1/2$). In the case of a half-filled band the t -model gives only one state (with zero energy). In the large U limit all the low energy states can then be described with an antiferromagnetic Heisenberg Hamiltonian which separates the different spin-states. The case with four electrons is especially easy to solve (see exercise 30.3. of Ref. [45]), leading to energy levels shown in Table II. The table also shows the orbital angular momentum determined from the symmetry properties of the Heisenberg state.

In the case of a large U the magnetic flux does not have any effect if $N = L$ due to the fact that the electron motion is strongly hindered. The situation changes if

TABLE II: Energy states of a Heisenberg ring with four electrons, sorted according to the spin S and total angular momentum M quantum numbers. M is determined with the help of the symmetry of the state.

S	S_z	M	E
0	0	2	$-2J$
0	0	0	$-J$
1	-1,0,1	0	0
1	-1,0,1	1	0
1	-1,0,1	3	0
2	-2,-1,0,1,2	2	J

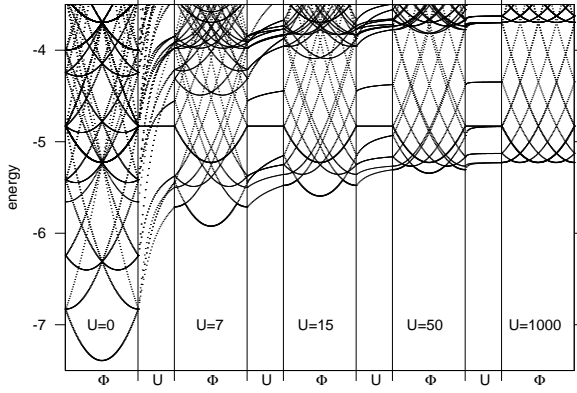


FIG. 9: Flux and U dependence of the many-body states of the Hubbard model with $N = 4$ and $L = 8$. For each fixed U the flux goes from 0 to Φ_0 ; in between, $\Phi = 0$ and U increases linearly to the next fixed value. The lowest overall energy and the lowest energy state corresponding to the maximum spin are shown as thick lines. Note that the maximum spin state is independent of U and that the periodicity of the yrast state changes from Φ_0 to $\Phi_0/4$ when U increases from 0 to ∞ .

empty sites are added. Figure 9 shows the development of the low energy states as a function of the magnetic field and U in the case of four electrons in eight sites. When U is reduced from infinity, the different spin-states separate, causing the periodicity of the yrast line to change from Φ_0/N at $U = \infty$ to Φ_0 at $U = 0$. This change of the periodicity is addressed in more detail in Sec. XII.

The effect of finite, but large U , is to split the degeneracy of the different spin-states of the t -model. If there are no empty sites, the Hamiltonian approaches that of the tJ -model, Eq. (63). We have solved the spectrum of four electrons as a function of the flux, increasing the number of sites from 4 to 12. The results show that when the number of empty sites increases, the spectra are still in fair agreement with those of the tJ -Hamiltonian, but the effective coupling between the spins, J , is not any more $4t^2/U$, but decreases rapidly when the number of empty sites increases.

Figure 10 shows the difference of the energy spectra derived from the exact Hubbard spectrum and from the t -model, for different values of empty sites. The results are scaled so that the energy difference between the two spin states corresponding to $M = 0$ are the same. We can

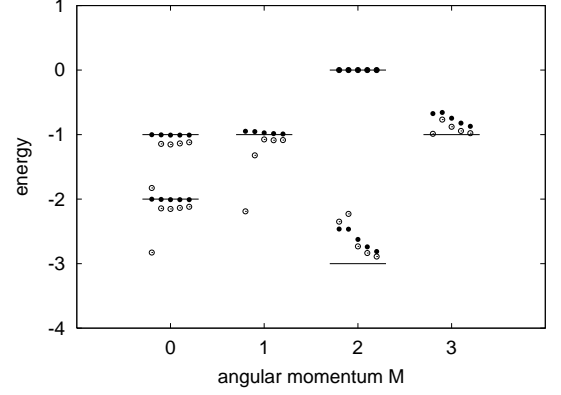


FIG. 10: The Heisenberg model energy spectrum for four electrons determined from the Hubbard model with empty sites. The black dots are the results for four electrons with $U = 100$ and different number of sites: For each state the dots from left to right correspond to $L = 5, 6, 8, 10,$ and 12 , respectively. For comparison, the solid lines denote the half-filling case (no empty sites), i.e. $L = 4$. In each case the energy difference of the two $M = 0$ states is adjusted to be 1. Open circles show the same for $U = 10$.

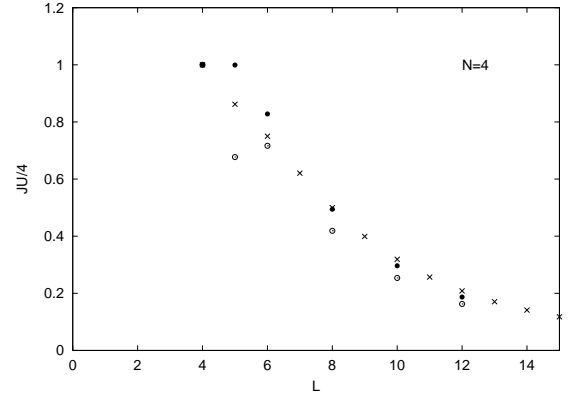


FIG. 11: The dependence of the effective Heisenberg coupling J on the number of sites (L). The crosses show the asymptotic large U limit of Eq. (64), the black dots (open circles) the result determined from the exact solution for $U = 100$ ($U = 10$).

see that when the number of empty sites increases, the difference spectrum approaches that of the Heisenberg Hamiltonian. These results suggest that the separation of the Hubbard Hamiltonian (for large U) into the t -model and Heisenberg Hamiltonians is accurate in the two limits, $N/L \rightarrow 1$ and $N/L \rightarrow \infty$. Moreover, the agreement with *all* numbers of empty sites is surprisingly good, even if U is as small as 10.

Yu and Fowler[55] have used the Bethe ansatz to study the large U limit for any number of empty sites and shown that the effective J_{eff} is related to the quantum numbers

k_j as

$$J_{\text{eff}} = \frac{4}{LU} \sum_{j=1}^N \sin^2 k_j. \quad (64)$$

Figure 11 shows the effective coupling constant determined by this equation as a function of the number of sites for a four electron ring, compared to those obtained from the direct diagonalization of the Hubbard Hamiltonian for $U = 10$ and $U = 100$. The agreement is fairly good for any number of empty sites even for the relatively small $U = 10$. The decrease of J_{eff} as a function of L can be explained with electron 'localization': When the number of empty sites increases, the localized electrons move further apart reducing the exchange interaction. We find, once again, that in the 1D system the electrons with repulsive (even δ -function) interactions behave as localized particles.

X. QUASI-1D-CONTINUUM RINGS: EXACT CI METHOD AND EFFECTIVE HAMILTONIAN

In this section we review electronic structure calculations for quasi-1D rings, published in Refs. [46, 47]; they were a natural continuation of earlier calculations done for electrons in harmonic two-dimensional quantum dots[37]. Usually the quantum ring is described with a displaced harmonic confinement (although several other models have been used[69, 70])

$$V(r) = \frac{1}{2}m_e\omega_0^2(r - r_0)^2, \quad (65)$$

where r_0 is the radius of the ring and ω_0 the perpendicular frequency of the 1D wire. Note that we still assume the ring to be strictly two-dimensional, i.e. it is infinitely thin in the direction perpendicular to the plane of the ring. The parameters describing the ring, r_0 and ω_0 can be related to the density parameter $r_s = 1/(2n_0)$ of the 1D system (n_0 is the 1D density) and to a parameter describing the degree of one-dimensionality of the wire. For the latter, Reimann *et al.*[46, 71] used a parameter C_F defined with the relation $\hbar\omega_0 = C_F\hbar^2\pi^2/(32mr_s^2)$. The physical meaning of C_F is that it is the ratio of the first radial excitation in the ring to the Fermi energy (approximated by that of an ideal 1D Fermi gas with the same density) of the 1D electron gas.

There are several approaches to solve the many-body problem of interacting electrons in the above potential. In studying the spectral properties the most useful method is the brute force diagonalization of the many-body Hamiltonian in a proper basis. This Configuration-Interaction (CI) method gives the whole many-body energy spectrum as well as the corresponding many-body states. Naturally, the solution can be numerically accurate only for small numbers of electrons, typically less than 10. The matrix dimension can be reduced by fixing the orbital angular momentum to the desired value.

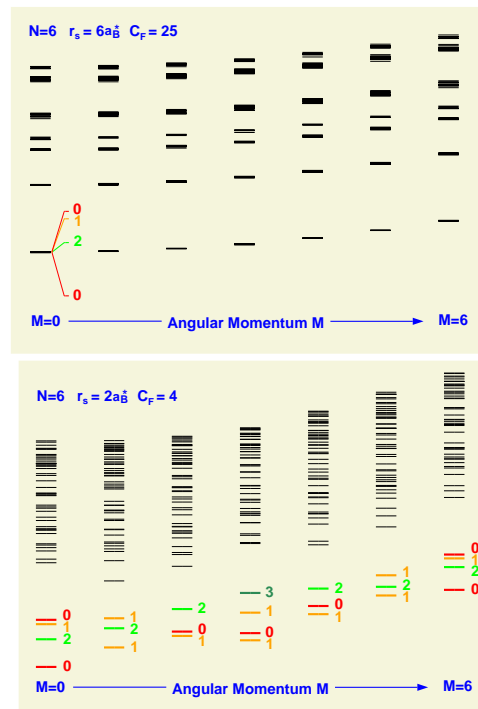


FIG. 12: Energy spectra for two quasi-one-dimensional continuum rings with six electrons (in zero magnetic field). The upper panel is for a narrow ring and it shows several vibrational bands. The lower panel is for a wider ring which shows stronger spin separation of energy levels corresponding to different spin states (shown as numbers next to the energy levels). Note that also the narrow ring has the same spin-ordering of the nearly degenerate state as expanded for the lowest $M = 0$ state.

For example, Koskinen *et al.*[46] first expanded the solutions of the single particle part of the Hamiltonian in a harmonic oscillator basis and then used these functions as a single particle basis for the Fock space in doing the CI calculations. According to their eigenenergies, up to 50 single-particle states were selected to span the Fock space and the number of the many-body Fock-states was restricted to about 10^5 using another energy cutoff (for a given total M). For an even number of electrons all spin-states can be obtained with fixing $N_{\uparrow} = N_{\downarrow} = N/2$. The total spin of each state can afterwards be determined by calculating the expectation value of the \hat{S}^2 operator.

Figure 12 shows the calculated energy spectra obtained with such a calculation for two different rings with six electrons in each. It is instructive to introduce a simple model Hamiltonian[46]

$$H_{eff} = \frac{\hbar^2}{2I}\mathbf{M}^2 + \sum_{\nu} \hbar\omega_{\nu}n_{\nu} + J \sum_{\langle i,j \rangle} \mathbf{S}_i \cdot \mathbf{S}_j \quad (66)$$

where ω_{ν} are the frequencies and the integers n_{ν} the number of excitation quanta of the various vibrational normal modes, and I is the moment of inertia of the 'molecule'. This Hamiltonian is thus simply a combination of rigid rotation of the whole system, internal vibration, and a

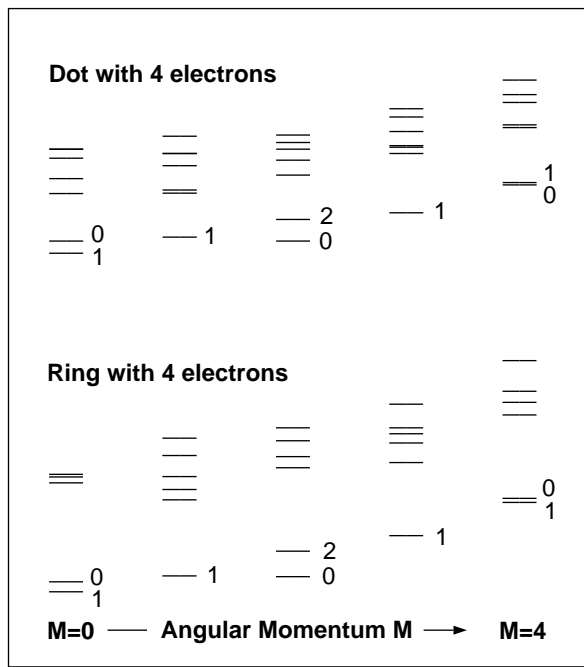


FIG. 13: Low energy spectra of a four electron quantum dot (upper panel) and a four electron quantum ring (lower panel) as a function of the angular momentum. The numbers next to the energy levels give the total spin. CI calculation from [72].

Heisenberg term to capture the spin dynamics, and one may examine how well it describes the exact results. To this end, note the following interesting features in Fig. 12: The narrower ring shows clear rotation-vibration bands, very similar to those obtained for electrons in a continuum ring with δ -function interaction, cfr. Fig. 5. The only difference is that now the ratios of the vibrational states correspond to those determined for classical electrons interacting with $1/r$ interaction.

Each spectral line consists of several nearly degenerate spin-states. The inset shows as an example the detailed structure of the $M = 0$ state. The spin structure coincides with that determined from the tJ -model, i.e. it can be determined by solving the antiferromagnetic Heisenberg model for a ring of six electrons. The ratios of the energies of different spin-states are quantitatively the same as in the Heisenberg model.

The lower panel of Figure 12 shows that this is true also for a wider ring. In this case only the vibrational ground state is clearly separated from the rest of the spectrum. However, the internal structure of this yrast band is still very close to that of the Heisenberg model: Qualitatively the agreement is exact, i.e. each angular momentum has the right spin states in the right order. Only the energy ratios are not any more exactly the same as in the Heisenberg model. Koskinen et al.[47] have studied in more detail how well the model Hamiltonian (66) describes the exact many-body results for a ring of six electrons.

Exact CI calculations for a ring of 4[72], and 5 and 7[46] electrons show similar agreement. Figure 13 shows the energy spectra for a four electron ring with a comparison to a four electron dot. With such a small number of electrons even the dot shows nearly the same yrast spectrum as the ring. This indicates that also in the dot the electrons will localize in a square Wigner molecule (see also [73]). Similar localization of electrons and their rotational and vibrational spectra are observed also in two-electron quantum dots[74] (where the energy spectrum can be solved exactly[75]). When the number of electrons in a quantum *dot* is 6 or larger the classical configuration of electrons in the Wigner molecule[76] is not any more a single ring and the spectral properties become more complicated. Nevertheless, even there the polarized case shows rotational bands consistent with the localization of electrons[77]. We should point out that the idea of describing few-electron systems in terms of rigid rotation and internal vibrations, is not new, but was first applied to quantum dots by Maksym[42].

XI. EXACT DIAGONALIZATION: FINITE MAGNETIC FIELD

Flux inside the ring

Let us first consider a magnetic field concentrating in the center of the ring, as described with the vector potential (14). Since the r -component of the vector potential is zero and the φ -component is proportional to $1/r$, the only effect of the flux is to change the angular momentum term of the single particle Schrödinger equation as

$$\frac{\hbar^2 m^2}{2m_e r^2} \rightarrow \frac{\hbar^2 (m - \Phi/\Phi_0)^2}{2m_e r^2}. \quad (67)$$

It is easy to see that for integer Φ/Φ_0 the energy levels and single particle states are equivalent to those without the flux, they are just shifted to another angular momentum value. Since each Slater determinant of the many-body state has a good angular momentum quantum number, the same is true for the many-body state: The angular momentum M is shifted to that of $M - N\nu$ when a integer number $\nu = \Phi/\Phi_0$ of flux quanta is penetrating the ring (as in Eq. (17) for a strictly 1D ring). This means that we get the same picture as discussed before: The effect of the increasing flux is just to tilt the spectrum so that successively higher and higher angular momentum values become the ground state. The ground state energy will be periodic with flux: $E_M(\Phi) = E_{M+N\nu}(\Phi + \nu\Phi_0)$. Note that this is true even if the M -dependence of the many-body spectrum is not exactly proportional to M^2 ; the only requirement is that the flux is restricted in the central region of the ring and the magnetic field does not overlap with the single particle states. In this case we can write the model Hamiltonian describing the yrast

spectrum of the exact CI calculation as

$$H = J \sum_{\langle i,j \rangle} \mathbf{S}_i \cdot \mathbf{S}_j + \frac{\hbar^2}{2Nm_e R^2} \left(M - \frac{N\Phi}{\Phi_0} \right)^2. \quad (68)$$

The observed periodicity of the ground state energy, or persistent current, as a function of flux is determined by the variation of the yrast-line as a function of M , for example as shown in Fig. 12. If the situation is like in the upper panel of Fig. 12, i.e. when the ring is very narrow, the energy increases accurately as M^2 . In this case Eq.(68) gives the periodicity Φ_0/N . On the other hand in the case of the lower panel of Fig. 12 the minimum energy jumps from $M = 0$ to $M = 3$ and then to $M = 6$, when the flux is increased. This means a periodicity of $\Phi_0/2$. If the ring is made even wider, eventually the minimum at $M = 3$ will not be reached and the periodicity changes to Φ_0 .

Finally, we should notice that if the electron gas were polarized (spinless electrons), the periodicity would always be Φ_0 . This can be seen from Fig. 12 which shows that the maximum spin state occurs in the lowest vibrational band only at the angular momentum $M = 3$ (more generally, at $M = N/2$ for even number of particles and at $M = 0$ for odd number of particles).

Homogeneous magnetic field, no Zeeman splitting

Experimentally it would be easier to measure the quantum rings in the presence of a homogeneous magnetic field. This case was first treated by first principle calculation methods in the pioneering papers by Chakraborty and Pietiläinen[78] and by Niemelä et al[70], and the present section is mainly based on these papers. In this case the vector potential can be expressed, for example, in terms of a symmetric gauge $\mathbf{A} = \frac{1}{2}(-By, Bx, 0)$. This vector potential effectively adds an additional harmonic confinement centered at the origin. The r -dependent single particle potential changes as

$$\frac{1}{2}m_e\omega_0^2(r - r_0)^2 \rightarrow \frac{1}{2}m_e\omega_B^2(r - r_B)^2 + \text{constant} \quad (69)$$

where $\omega_B^2 = \omega_0^2 + e^2 B^2 / (4m_e^2)$ and $r_B = r_0 \omega_0^2 / \omega_B^2$. The effect of the field is then just to change the parameters of the confining ring. This will change the energy differences between the single particle states, but as long as the ring is narrow enough to have only one radial mode, it can not change their order. Consequently, in narrow rings the effect of the field on the many-body state is small and only quantitative. Nevertheless, the change of the potential shape and the constant term means that the lowest single particle state increases with the flux[78], as shown in Fig. 14 for spinless electrons. The figure also indicates that the effect of the electron-electron interactions in the spinless case is mainly to shift the spectrum upwards by a constant.

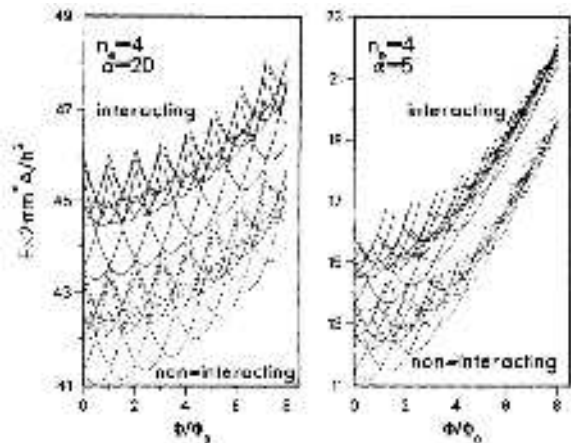


FIG. 14: Energy levels for four noninteracting (dashed lines) and interacting (solid lines) spinless electrons in a ring as a function of the magnetic flux. The magnetic field is homogeneous. From Ref. [78].

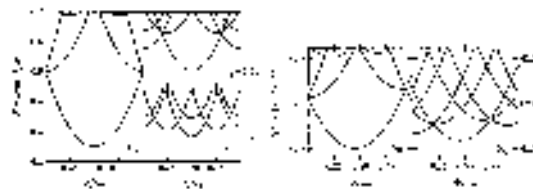


FIG. 15: Energy levels as a function of the magnetic flux in a ring of four electrons. The left-hand side shows the results for delta-function interaction in a strictly 1D ring, (a) for noninteracting, (b) and (c) for interacting so that in (c) the interaction is twice as strong as in (b). The right hand panel shows the result for a quasi-1D ring with $1/r$ -interaction, (c) noninteracting and (d) interacting electrons. Note the similarity of the results in (b) on the left-hand side and (d) on the right hand side. From Ref. [70]

Niemelä *et al.*[70] have performed an extensive study of quasi-1D-rings with 2 to 4 interacting electrons. They used a homogeneous magnetic field and neglected the Zeeman splitting. The results for two and three interacting electrons show periodicities $\Phi_0/2$ and $\Phi_0/3$, respectively, i.e. consistent with the Φ_0/N periodicity for a narrow ring. In the case of four electrons Niemelä *et al.* studied in addition to the $1/r$ Coulomb interaction also a δ -function interaction ($V_0\delta(r)$) in the case of an infinitely narrow ring. It is then interesting to compare the results of these two models, as shown in Figure 15. For the δ -function interaction the results are expected to be the same as for the Hubbard model with an infinite number of lattice sites. Indeed, the results show the change of periodicity from Φ_0 first to $\Phi_0/2$ and then to $\Phi_0/4$, when the strength of the δ -function interaction (V_0) is increased. The results of Fig. 15 compare well with the results of the Hubbard model with only 8 sites, i.e. those shown in Fig. 9 for $U = 0$, $U = 15$ and $U = 50$.

The right hand side of Fig. 15 shows the energy levels for a quasi-1D-ring with $1/r$ -interaction. The spectra are essentially the same, the only difference being a slight upward shift of the energy when the flux changes from 0 to 1. This is due to the harmonic repulsion of the flux-dependent effective potential, Eq. (69), caused by the homogeneous magnetic field. Note the similarities of the spectra shown in Figs. 15 b and c.

XII. PERIODICITY OF PERSISTENT CURRENT

A. Strictly 1D rings: Spectrum of rigid rotation

The many-electron excitation spectrum for electrons interacting with the infinitely strong δ -function interaction was studied using the Hubbard model in Sec.IX, see Fig. 7. As mentioned, this spectrum can be constructed from the Bethe ansatz. In the low-energy part of the spectrum (close to the yrast line) the levels consist only of the compact states of the quantum numbers I_j , i.e. there is no vibrational energy. It is instructive to use the continuum limit ($L/N \rightarrow \infty$) of the Bethe ansatz solution for the t -model to compare these (yrast) energy levels as a function of the flux Φ to those of *single* electron states in a ring of radius R . One finds for a many-electron state

$$E(M, \Phi) = \frac{\hbar^2}{2Nm_e R^2} \left(M - \frac{\Phi}{h/Ne} \right)^2 \quad (+constant) \quad (70)$$

and for a single electron state

$$\epsilon(m, \Phi) = \frac{\hbar^2}{2m_e R^2} \left(m - \frac{\Phi}{h/e} \right)^2 \quad (71)$$

where we have now written the flux quantum as $\Phi_0 = h/e$. We notice that the many-electron states are identical to the single electron levels with the electron mass and charge, m_e and e , replaced by the total mass and total charge of all the electrons, Nm_e and Ne . Indeed the strongly correlated electron system with infinitely strong delta function interaction behaves as a rigidly rotating single particle. We should note that in the spinless case the number p of Eq.(39) is always zero and consequently one recovers the noninteracting case (for spinless electrons the δ -function interaction does not have any meaning due to the Pauli exclusion principle). The rigid rotation of the electron system then leads always to the Φ_0 periodicity as discussed already in Sec.III

We have learned in Secs. X and XI on the basis of numerical solutions for narrow quasi-1D rings, that electrons with normal $1/r$ interactions also produce similar rotational spectrum. Moreover, the solution of the Calogero-Sutherland model shows rigorously that a similar spectrum is observed for $1/r^2$ -interaction. Both these interactions have the property that they are infinitely

strong at the contact, preventing the electron to pass each other. It seems obvious that any repulsive interaction which is infinitely strong (in such a way that electrons with opposite spin are not allowed at the same point) produces for the strictly 1D ring the same spectrum of rigid rotation.

The yrast spectrum is qualitatively similar for all electron numbers. In particular, in experimentally determined spectra, the number of electrons in the ring can be seen as a qualitative change of the spectrum only by observing the vibrational bands. (The yrast energy alone determines the number of electrons in a narrow ring only if the flux is quantitatively determined.) A way of estimating the number of particles is to count the number of (purely rotational) states below the onset of the first vibrational band, as can be seen from the following argument: By considering noninteracting spinless electrons (which have exactly the same energy levels, though not all of them, as spinful electrons) we know from Eq.(5) that the first vibrational level is the first noncompact state, having an excitation energy of about $N\hbar^2/2m_e R^2$. This equals the $E(M = N, \Phi = 0)$ energy of the yrast band, Eq.(70). For N particles there are thus about N purely rotational states below the first vibrational band. Figure 7 demonstrates that this is true for $N = 4$.

B. Periodicity change in quasi-1D rings

In this section we will concentrate on the lowest energy state (the yrast state) and study in more detail its periodicity in quasi-1D rings, where the electrons are allowed to pass each other. (The periodicity of the persistent current at zero temperature is the same as that of the ground state energy). As discussed in Sec. IX F, the (strictly 1D) Hubbard model suggests that (i) for spinless electrons the periodicity is always the flux quantum Φ_0 and (ii) for electrons with spin the periodicity changes from Φ_0 first to $\Phi_0/2$ and then to Φ_0/N when the interaction U increases from zero to infinity, as illustrated in Fig. 9. This change of periodicity in the Hubbard model was first studied by Yu and Fowler[55] and Kusmartsev *et al.*[79].

The change in periodicity can be traced back to the notion that the Hubbard model with empty sites can be quite accurately described by the tJ_{eff} -model with an effective exchange coupling J_{eff} which depends not only on U but also on the number of empty sites, as demonstrated in Figs. 10 and 11. When J_{eff} is small, the Φ_0/N periodicity is observed, while for large J_{eff} the Φ_0 periodicity is found (for even numbers of electrons). The periodicity of $\Phi_0/2$ results from the fact that the solution of the Heisenberg Hamiltonian has two close lying states corresponding to angular momenta $M = N/2$ and $M = 0$, while the states corresponding to other angular momenta are clearly higher in energy. The situation is demonstrated in Fig. 16 where we show the energy spectrum for the Heisenberg model for an eight electron

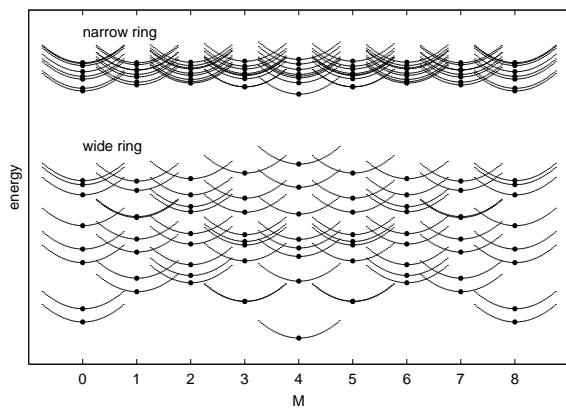


FIG. 16: Schematic illustration of the Φ_0/N and $\Phi_0/2$ periodicities of a ring with eight electrons. The black points show the energy spectra with two different values of J . The parabolas drawn at each point indicate the change of the rotational energy level as a function of the magnetic flux. The lowest envelope of the overlapping parabolas gives the ground state energy as a function of the flux.

ring. The energy spectrum for the total Hamiltonian as a function of the flux can be estimated simply by drawing a parabola at each energy level as shown in the figure. Now depending on the energy splitting of the Heisenberg model, i.e. on J_{eff} , the resulting lowest energy state as a function of flux can have periodicities, Φ_0/N , $\Phi_0/2$, or Φ_0 .

Deo *et al.*[80] have studied the periodicity change using the model Hamiltonian Eq.(68) which is known to give good agreement with exact diagonalization results of the quasi-1D continuum Hamiltonian. This model Hamiltonian has the same flux dependence as Eq.(70), which was derived from the Hubbard model. It is thus natural that the same periodicity change is observed. In both cases the flux only affects the rotational state of the system by changing its energy as $M^2 \rightarrow (M - N\Phi/\Phi_0)^2$, but does not change the *internal structure* of the many-body state in question, i.e. all interparticle correlations remain the same.

We can look at the periodicity change in more detail by making a Fourier analysis of the lowest energy state. We have done this using the model Hamiltonian (68). A parameter determining the relative weights of the energy states of the two separable parts of the Hamiltonian is then JI , i.e. the product of the moment of inertia ($I \approx Nm_e R^2$) and the Heisenberg coupling parameter (in the Hubbard model the corresponding parameter would be J_{eff}). Figure 17 shows the three most important Fourier components as a function of JI for rings with 6, 7 and 8 electrons. For 6 and 8 electrons we see clearly the period changes. In the case of an odd number of electrons, the solution of the Heisenberg model is qualitatively different: There are two degenerate minima corresponding to different angular momenta. Consequently, the period $\Phi_0/2$ stays always more important than the

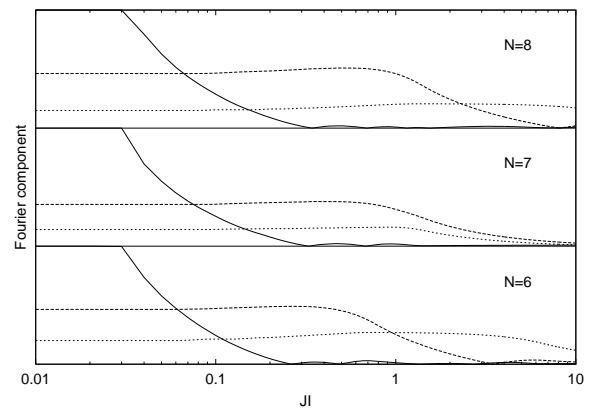


FIG. 17: Three largest Fourier components of the periodic ground state energy. JI is the product of the effective Heisenberg coupling and the moment of inertia. The dotted, dashed and solid lines are the Fourier components corresponding to the periodicities Φ_0 , $\Phi_0/2$ and Φ_0/N , respectively.

period Φ_0 [80].

We have learned that the periodicity change as a function of the effective width of the quasi-one-dimensional continuum ring is similar to that in a strictly 1D Hubbard ring as a function of U , suggesting that the finite U in the Hubbard model mimics the finite width of a continuum ring. This similarity can be understood as follows. With infinite U the electrons are forbidden to pass each other. This situation is similar to an infinitely narrow continuum ring with $1/r$ interaction between the electrons. When U gets smaller, the electrons (with opposite spin) can hop over each other, the better the smaller U is. Naturally, in the continuum ring the electrons are allowed to pass each other if the ring has a finite width. Decreasing U in the Hubbard model thus corresponds to making the continuum ring wider.

Note that in order to see the periodicity in the Hubbard model, one has to consider systems where the number of electrons N is smaller than the number of lattice sites L , i.e. empty sites are needed for 'free rotation' of the ring. The resulting periodicity depends both on the number of empty sites and on the on-site energy U .

XIII. OTHER MANY-BODY APPROACHES FOR QUASI-1D CONTINUUM RINGS

Quantum monte carlo

A class of powerful tools to study the low energy states of many-body quantum systems are based on the Monte Carlo method[81]. These methods have been extensively applied also for quantum dots[82, 83, 84, 85, 86] and quantum rings[87, 88] with a few electrons. Monte Carlo approaches are most suitable for studying either the ground state properties (variational Monte Carlo and diffusion Monte Carlo) or average finite temperature prop-

erties (path integral Monte Carlo), and have thus not been able to produce the detailed spectral properties with the accuracy of the CI method. It also seems that even finding the correct ground state is not straightforward by using Quantum Monte Carlo[89]

Pederiva *et al.*[88] have used so-called fixed-node diffusion Monte Carlo for studying six electron quantum rings. They calculated also the lowest excited states for $M = 0$. They found the ground state to have $S = 0$ and the first excited state $S = 2$, in agreement with the CI calculations and the Hubbard model, while for the second and third excited states they obtained the $S = 1$ and $S = 0$ states in opposite order as compared to the CI calculations. Nevertheless, as the authors note, the energy differences in the narrow rings are so small that their difference starts to be within the statistical accuracy of the Monte Carlo method.

The Monte Carlo studies for small quantum dots and rings show that while these methods can predict accurately the ground state energy, they are not yet capable to give reliably the salient features of the many-body spectrum.

Local density approximation

The density functional Kohn-Sham method is another approach mainly suitable for the determination of the ground state structure. In applications to quantum dots and rings (for a review see [37]), the local spin-density approximation (LSDA) is usually made and the system is assumed to be strictly two-dimensional. Generally, the Kohn-Sham method is a 'mean field' method, where the electron-electron correlation is hidden in an effective single particle potential. This causes the interesting feature that the mean field can exhibit symmetry breaking and the total electron and spin densities can reveal the *internal* symmetry of the ground state, for example the internal shape of nucleus or atomic cluster[90] or the static spin-density wave in a quantum dot[91]. Indeed, in applications to quantum rings, the LSDA indicated the localization of electrons in an antiferromagnetic ring[71]. Nevertheless, we should add that although the LSDA can often elucidate the internal structure of a rotating system, the method is not foolproof: In some cases, for example in rings or dots with high enough electron density, it will not break the symmetry.

Systematic studies of quantum rings in terms of density functional methods have been performed in several papers [92, 93, 94, 95], and comparisons with 'exact' many-body methods show that the LSDA gives accurately the ground state energy[88]. The LSDA has been extended to so-called current-spin-density functional theory (CS-DFT) which can take into account the gauge field[96]. Viefers *et al.* have applied the CS-DFT for studying the persistent current, i.e. the ground state energy as a function of the magnetic field, in small quasi-1D quantum rings. For a four electron ring (with $r_s = 2.5$, $C_F = 10$)

they found the yrast line consisting of two states: At zero flux (and at $\Phi = \Phi_0$) the ground state had $S = 1$ while around $\Phi = \Phi_0/2$ the ground state had $S = 0$. These results are in agreement with the CI calculations and the results of the Hubbard model for four electrons. Similar agreement was found for a six electron ring. The spin-densities showed a clear localization of electrons in an antiferromagnetic ring.

Density functional theory has the same problem as quantum Monte Carlo in that the determination of excited states is not straightforward (although time-dependent current-spin-density-functional theory can provide some information on excitations[92, 93, 95]). Consequently, it is not possible to construct the complete excitation spectrum as by using the brute force CI method.

XIV. RELATION TO LUTTINGER LIQUID

Infinitely long one-dimensional systems are often studied as Luttinger liquids[97, 98] (for reviews see [5, 6, 7]). The speciality of the strictly 1D systems arises from the fact that the Fermi surface consists of only two points ($\pm k_F$). This leads to a Peierls instability[99] and a breakdown of the Fermi liquid theory in a strictly 1D system. Important low energy excitations will then be collective, of bosonic nature, and have a linear dispersion relation. The Luttinger liquid also exhibits so-called charge-spin separation: The spin and charge excitations can move with different velocities. In addition to studying the low energy excitations, the Luttinger model has been extensively used for studying correlation functions[6, 8].

It has been shown that the tJ -model is a Luttinger liquid[6]. In the limit of a narrow ring with many electrons the spectral properties of the quantum rings must then approach those of a Luttinger liquid. We will now demonstrate that the many-body spectra of quantum rings are consistent with the properties of the Luttinger liquid. We do this only by qualitative considerations. In an infinitely long 1D system, the low energy single particle excitations (of free fermions) are restricted to have a momentum change of $q \approx 0$ due to the fact that the Fermi surface is a point. In the Luttinger model it is precisely these excitations that lead to the bosonization and collective plasmon excitations[6] with a linear dispersion relation. In the case of a finite ring these single particle excitations are just those described in Fig. 1, where one of the last electrons is excited from the compact state (or similarly in the Bethe ansatz solution of the t -model). Now, it is exactly these single particle excitations which lead to the vibrational model, i.e. longitudinal acoustic phonons in the limit of a long ring (see Fig. 4), which have a linear dispersion relation (for small q). The excitation spectrum is in qualitative agreement with the prediction of the Luttinger model already in the smallest rings.

Casting the Hamiltonian explicitly into charge de-

pendent parts (rotations and vibrations) and a spin-dependent part (Heisenberg Hamiltonian), as in Eqs.(13) and (66) is equivalent to the charge-spin separation in the Luttinger model. In an infinite system this can be explicitly done for the half-full Hubbard model ($L = N$). We have demonstrated in Sec. IX F that the spin degrees of freedom can be described with a good accuracy with the Heisenberg model in a much larger variety of quasi-1D rings.

XV. PAIR CORRELATION

The internal structure of a many-body electron state, especially the possible localization to a Wigner molecule, can be studied by examining the correlation functions. We have done this already for non-interacting electrons in Fig. 3 where we used the N -particle correlation function for identifying the vibrational states. The N -particle correlation function is just the square of the normalized many-body wave function. A related analysis of the maximum N -particle correlation for the Hubbard model, in Table I, also revealed the internal structure of the vibrational states.

The pair correlation function is frequently used to study the internal structure of a many-body state. In one-dimensional systems the pair-correlations have the property that they decay with distance as $1/r^\alpha$ [8]. Consequently, the 1D electron system does not have a Wigner crystal with true long-range order. The same is true for the spin-density oscillations: For example in the antiferromagnetic Heisenberg model in 1D the spin-spin correlation decays as $1/r$, r being the distance between the electrons.

In finite 1D rings, with only a few electrons, the pair correlation function is even less informative. The reason is again the Pauli exclusion principle, which prevents electrons with the same spin to be at the same site. This means that within a short distance, the pair correlation functions are quite insensitive on the electron-electron interaction. This is demonstrated in Fig. 18 where we show the calculated pair correlation function for two different continuum rings[100] and compare them to the pair correlation of the Heisenberg model. We have also studied the pair correlation for four electrons using the t -model and found that the correlation is independent of the number of empty sites, as expected from the notion (Section IX F) that the spin-spin correlation is determined from the Heisenberg model, whatever the number of empty sites.

The effect of temperature on the pair correlation function has been studied by Borrmann and Harting[87] using quantum Monte Carlo. Koskinen *et al.*[47] used the model Hamiltonian (66) to determine the temperature dependence by calculating separately the pair correlation for each quantum state. Both methods agree in the fact that the correlations between the electrons vanish as soon as the temperature exceeds the first excited state of

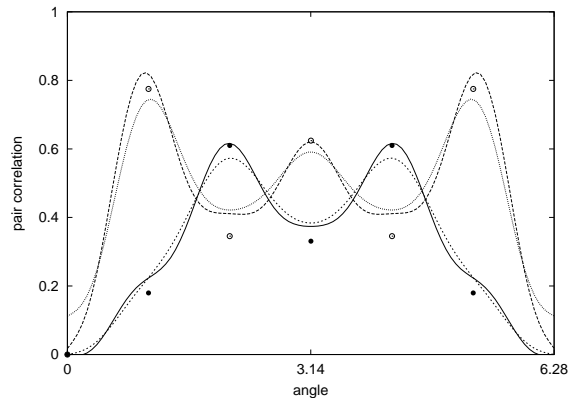


FIG. 18: Pair correlation function for six electrons in a quasi-one-dimensional continuum ring, calculated with the CI method. Solid and long-dashed lines: $\uparrow\downarrow$ -correlation and $\uparrow\uparrow$ -correlation, respectively, for a narrow ring with $r_s = 2$ and $C_F = 25$. Dashed and dotted lines: $\uparrow\downarrow$ -correlation and $\uparrow\uparrow$ -correlation, respectively, for a wider ring with $r_s = 2$ and $C_F = 4$. The filled and open circles show the correlations for a six electron antiferromagnetic Heisenberg ring. The functions are normalized so that the integral of the $\uparrow\downarrow$ -correlation is 3 and that of the $\uparrow\uparrow$ -correlation is 2.

the system.

XVI. INTERACTION OF THE SPIN WITH THE MAGNETIC FIELD: THE ZEEMAN EFFECT

Throughout most of this paper we have assumed that the magnetic flux is confined inside the ring so that the electrons move in a field-free region. Experimentally, however, it might be difficult to produce a situation where the magnetic field is zero at the ring site (or the effective Landé factor is zero). It is then important to consider also the Zeeman effect when comparing theory with experiments. The interaction between the electron spin and the magnetic field adds to the Hamiltonian a term $\mu_B g_0 S_z B$. In the case of a narrow ring it is beneficial to write this as[47]

$$H_Z = \frac{\hbar^2}{2m_e R^2} \left(\frac{\Phi}{\Phi_0} \right) g S_z, \quad (72)$$

where we have written the field with help of the flux, ring radius, and an effective Landé factor g . For example, in the case of a homogeneous magnetic field and an ideal 1D ring $\Phi = \pi R^2 B$, and $g = g_0$. The advantage of writing the Zeeman part of the Hamiltonian as above is that we can study continuously the change in the spectra when we move from the case (14), no Zeeman effect, to a homogeneous magnetic field simply by changing g . Moreover, the fact that the effective Landé factor in semiconductors differs from that of the free electron can also be taken into account by just changing g .

The periodicity of the persistent current, or lowest energy state, as a function of flux is caused by the ground

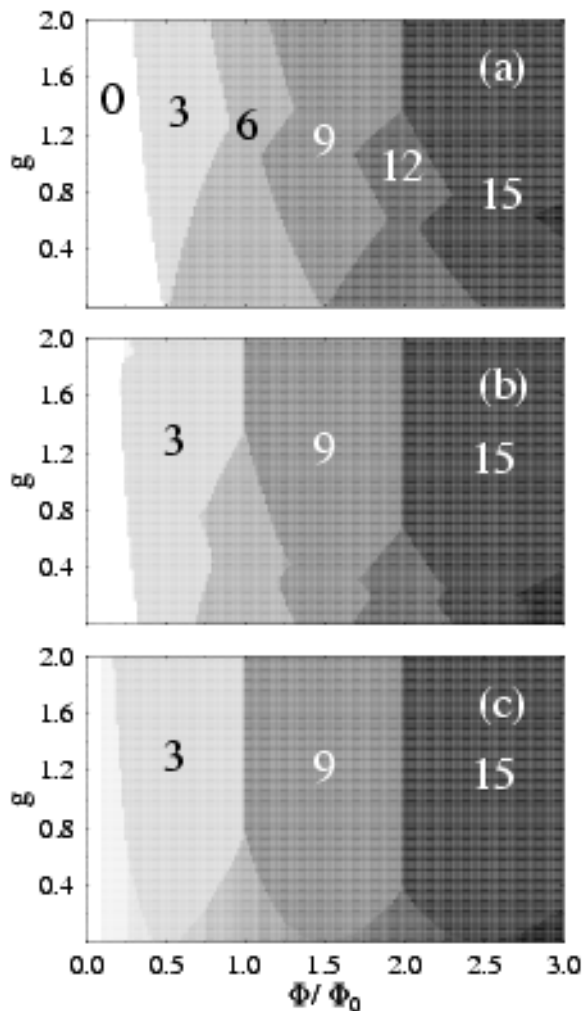


FIG. 19: Angular momentum of the ground state of a six electron ring as a function of the flux and the effective Lande factor g . The angular momentum is shown as numbers and it increases with the darkness of the grayscale. The uppermost panel is for $JI = 6$ in the model Hamiltonian (66), the center panel for $JI = 1.8$ and the lowest panel for $JI = 0$.

state energy jumping from one angular momentum state to another. If all possible angular momenta are visited (J_{eff} is small in the models discussed in Sec. IX F), the periodicity is Φ_0/N ; if angular momenta $M = 0, N/2, N$ etc. (or $N/2, 3N/2$ etc.) are visited the periodicity is $\Phi_0/2$, and if only angular momenta $M = 0, N, 2N$ etc. are visited the periodicity is Φ_0 . In order to determine the overall periodicity it is thus sufficient to examine the angular momentum values of the lowest energy state as a function of the flux.

Figure 19 shows the angular momentum of the ground state as a function of the flux and the effective Landé factor discussed above. The results are shown for three different values of the parameter J_{eff} . When the Landé factor approaches the free electron value $g = 2$ and the flux is large, the periodicity always becomes Φ_0 . The reason is

the large Zeeman effect which makes the maximum spin state $S_z = N/2$ the lowest energy state. This state has always the periodicity Φ_0 as shown in Fig. 9. In a wide ring (a) where the periodicity is Φ_0 for $g = 0$ it changes first to $\Phi_0/2$ and then again to Φ_0 when g increases. This is due to the fact that (in a ring of six electrons) angular momenta $M = 0, 6, \dots$ are the ground states for the nonpolarized case while for the polarized case the ground state angular momenta are $M = 3, 9, \dots$. In the transition region a periodicity $\Phi_0/2$ is observed. In the narrow ring (c) the periodicity changes smoothly from Φ_0/N to Φ_0 when g is increased from zero.

XVII. EFFECT OF AN IMPURITY

There has been extensive research on the effects of impurities on the persistent current. Already in 1988, Cheung *et al.* [101] used a simple tight binding model for studying the effect of disorder in 1D rings and found the decrease of the persistent current with increasing disorder. Chakraborty and Pietiläinen[102] used the CI method for studying the effect of an impurity in a polarized electron ring. The basic results of the included Gaussian impurity potential were to lift some of the degeneracies of the energy levels and decrease the persistent current. Similar findings were observed by Halonen *et al.*[103] in the case where the spin was included. The suppression of the persistent current due to a gaussian impurity was also computed by Viefers *et al.*[94] using density functional theory, thus including the effects of both spin, realistic interactions and finite width of the ring. Eckle *et al.*[59, 104] have used the Hubbard model to study the effect of coupling the quantum ring to a quantum dot at Kondo resonance. They have shown that at certain values of the flux the problem can be solved exactly using the Bethe ansatz.

The effect of an impurity is easy to study in the Hubbard model, where in the simplest case we can just add a repulsive or attractive potential in one of the lattice sites. Figure 20 shows how the flux dependence of the energy levels changes when a repulsive external potential is introduced in one of the lattice sites. The effect is to open gaps in the spectrum. The impurity potential splits the degeneracy of angular momenta (modulo 4) and makes all the energy levels oscillate with a period of Φ_0 instead of the period of $NL\Phi_0$ seen in the impurity-free case. Note, however, that the levels corresponding to different angular momenta still cross and the lowest energy state has the same period as without the impurity.

In the above example, the energy of the lattice site, say site number 1, was changed by introducing a term $\Delta(\hat{n}_{1\uparrow} + \hat{n}_{1\downarrow})$ in the normal Hubbard Hamiltonian, Eq. (32). Figure 21 shows how the lowest energy state as function of flux changes when Δ is varied from -20 to 20 in steps of 2. For a relatively small value of U ($=20$) and an attractive impurity, the variation of the ground state energy as a function of the flux is nearly independent of the

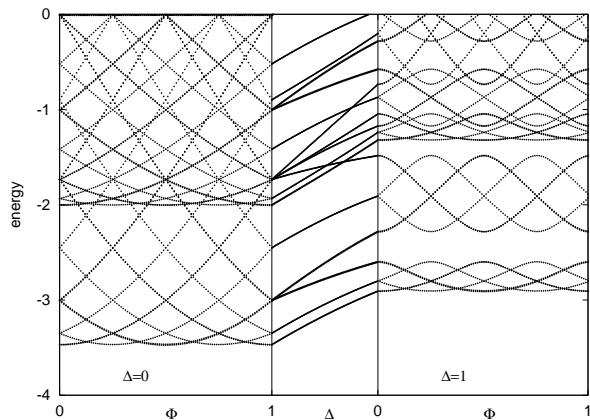


FIG. 20: Effect of an impurity on the energy levels of a six-site Hubbard ring with four electrons. The left panel shows the energy levels as a function of the flux (in units of Φ_0) for an impurity free ring. The middle panel shows the evolution of the energy levels at zero flux as a function of an impurity potential Δ at one of the lattice sites. The right panel shows the energy levels as a function of flux in the case where $\Delta = 1$. $U = 1000$ in all cases.

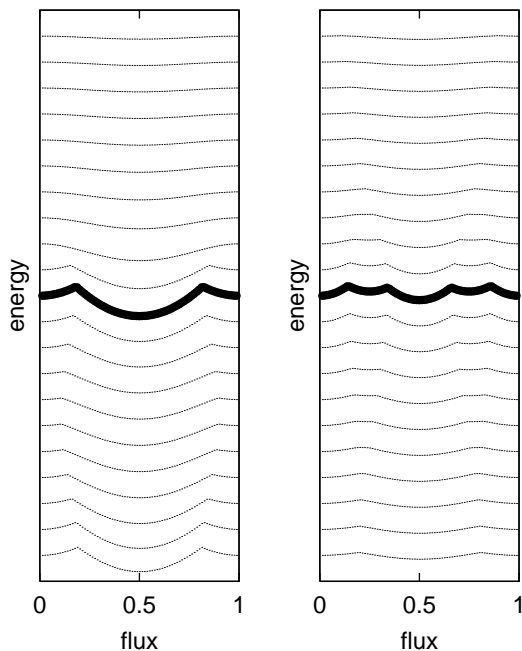


FIG. 21: Effect of an impurity on the lowest energy state in a Hubbard ring with $L = 6$ and $N = 4$. The left panel is for $U = 20$ and the right panel for $U = 200$. The thick line is the result without the impurity and the other lines correspond to rings where the energy of one lattice site is increased (see text) by 2, 4, 6, etc. (dotted lines above the thick line) or decreased by 2, 4, 6 etc. (dotted lines below the thick line). All lines have been shifted vertically so that they appear to be equally spaced. The energy scale in each line is the same, but it is twice as large for $U = 200$ as compared to $U = 20$. The flux is in units of $\Phi_0 = h/e$.

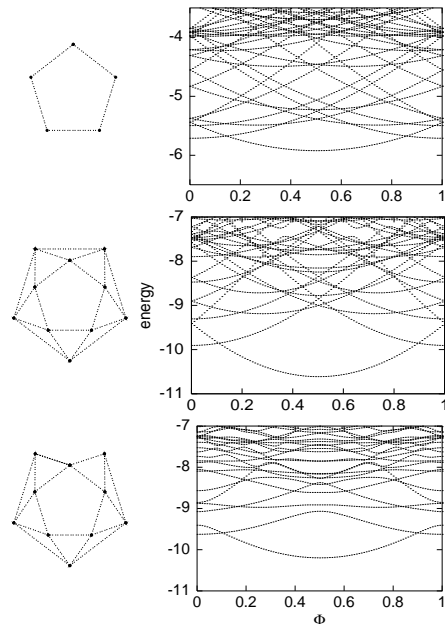


FIG. 22: Energy spectra as a function of flux for four electron clusters. Upper panel: Hubbard ring with five sites and finite $U = 7$. Middle panel: “Quasi-one-dimensional” t -model ring. Lowest panel: Quasi-one-dimensional t -model ring with a defect. The geometries in each case are shown at the left.

impurity potential, while a positive (repulsive) impurity potential reduces the amplitude of the oscillation, as expected from all earlier studies[70, 94, 102, 103]. Since the ground state persistent current is essentially the derivative of the energy wrt. flux, see Eq.(24), this directly reflects the suppression of the current. In the case of a relatively large U (in the present example $U = 200$), we see that the impurity potential changes the original periodicity Φ_0/N to $\Phi_0/2$.

In the case of small systems the Hubbard model can easily be used in studying also other kinds of impurities. For example, two impurities or even random potentials at lattice sites have qualitatively the same effect on a Hubbard ring as a single impurity, as shown in Fig. 20. The Hubbard model may furthermore be used to study the coupling of the ring to a quantum dot[59], as mentioned earlier. In Figure 22 we present another example demonstrating how the Hubbard model can be extended to quasi-1D rings with impurities. In the uppermost panel of the figure we show the energy spectrum of a 1D Hubbard ring with four electrons and a finite $U = 7$. The middle panel represents a *quasi*-1D ring with infinite U (t -model). Comparison of these two models shows that a finite U in a strictly 1D Hubbard model actually mimics well the quasi-one-dimensionality of a more realistic ring, as noticed already in comparing the Hubbard model with the continuum models. The lowest panel of Fig. 22 shows an ‘impurity’ or a narrow neck in the ring. Its effect is to open gaps in the excitation spectrum. Qualitatively, the effect is the same as observed above for a

1D Hubbard ring with an impurity potential.

In many experiments, the persistent current is measured for a collection of rings, possibly consisting of several propagating channels (radial modes). The persistent currents in such rings are not determined by quantum mechanical eigenenergies of a single ring, but are affected by several complications like disorder and ensemble averaging [105, 106, 107]. The electron-electron interactions seem to play a crucial role also in the disordered rings [108]. Müller-Groeling and Weidenmüller have shown that interactions effectively counteract the impurity suppression of the persistent current [109], in qualitative agreement with our Hubbard model results.

XVIII. SUMMARY

In this paper we have attempted to present a comprehensive review of the physics of few-electron quantum rings, with particular focus on their energy spectra and the periodicity of the persistent current. We compared various analytical and numerical theoretical approaches which fall into two main classes – lattice models on the one hand and continuum models on the other – and tried to clarify the connections between them. The main message is that all the different approaches give essentially the same results for the spectra and persistent currents

(provided one takes the continuum limit of the discrete models to compare them to the continuum ones). The essential physics is captured by a simple model Hamiltonian which describes the many-body energy as a combination of rigid rotation and internal vibrations of the ring ‘molecule’, plus a Heisenberg term which determines the spin dynamics. In the spectra, the vibrational excitations can be seen as higher bands, while the lowest (yrast) band is purely rotational. Its periodicity with respect to the flux is always Φ_0 in the case of spinless (polarized) electrons, while for a clean ring of nonpolarized electrons, the periodicity changes from Φ_0 via $\Phi_0/2$ to Φ_0/N as the ring get narrower or, in the language of the Hubbard model, as the interaction strength U increases (the effective Heisenberg coupling J decreases). Impurities in the ring may change the periodicity (to Φ_0) even in the nonpolarized case, and moreover suppress the persistent current.

Acknowledgements

We would like to thank M. Koskinen for enlightening discussions. This work has been supported by Nordita and by the Academy of Finland under the Finnish Centre of Excellence Programme 2000-2005 (Project No. 44875, Nuclear and Condensed Matter Programme at JYFL).

-
- [1] Y. Aharonov and D. Bohm, *Phys. Rev.* **115**, 485 (1959).
 - [2] M. Büttiker, Y. Imry, and R. Landauer, *Phys. Lett. A* **96**, 365 (1983).
 - [3] S. Tarucha, D.G. Austing, T. Honda, R.J. van der Haage, and L. Kouwenhoven, *Phys. Rev. Lett.* **77**, 3613 (1996).
 - [4] A. Lorke, R.J. Luyken, *Physica B* **256** 424 (1998)
 - [5] F.D.M. Haldane, in *Proceedings of the International School of Physics ‘Enrico Fermi’ Course CXXI*, North Holland (1994).
 - [6] J. Voit, *Rep. Prog. Phys.* **57**, 977 (1994).
 - [7] H.J. Schulz, in *Proceedings of Les Houches Summer School LXI*, ed. E. Akkermans, G. Montambaux, J. Pichard, et J. Zinn-Justin (Elsevier, Amsterdam, 1995).
 - [8] E.B. Kolomeisky and J.P. Straley, *Rev. Mod. Phys.* **68**, 175 (1996).
 - [9] J. Hubbard, *Proc. R. Soc. London A* **276**, 238 (1963).
 - [10] H. Bethe, *Z. Phys.* **71**, 205 (1931).
 - [11] E.H. Lieb and F.Y. Wu, *Phys. Rev. Lett.* **20**, 1445 (1968).
 - [12] C.L. Kane, preprint, cond-mat/0210621.
 - [13] J.M. Garcia, G. Medeiros-Ribeiro, K. Schmidt, T. Ngo, J.L. Feng, and A. Lorke, *Appl. Phys. Lett.* **71**, 2014 (1997).
 - [14] A. Lorke, R.J. Luyken, A.O. Govorov, J.P. Kotthaus, J.M. Garcia, and P.M. Petroff *Phys. Rev. Lett.* **84** 2223 (2000).
 - [15] R. A. Webb, S. Washburn, C. P. Umbach, and R. B. Laibowitz, *Phys. Rev. Lett.* **54**, 2696 (1985).
 - [16] L.P. Lévy, G. Dolan, J. Dunsmuir, and H. Bouchiat, *Phys. Rev. Lett.* **64**, 2074 (1990).
 - [17] V. Chandrasekar, R.A. Webb, M.J. Brady, M.B. Ketchen, W.J. Gallagher, and A. Kleinsasser, *Phys. Rev. Lett.* **67**, 3578 (1991).
 - [18] G. Timp, A. M. Chang, J. E. Cunningham, T. Y. Chang, P. Mankiewich, R. Behringer, and R. E. Howard, *Phys. Rev. Lett.* **58**, 2814 (1987).
 - [19] C. J. B. Ford, T. J. Thornton, R. Newbury, M. Pepper, H. Ahmed, D. C. Peacock, D. A. Ritchie, J. E. F. Frost, and G. A. C. Jones, *Appl. Phys. Lett.* **54**, 21 (1989).
 - [20] G. Timp, P. M. Mankiewich, P. deVegvar, R. Behringer, J. E. Cunningham, R. E. Howard, and H. U. Baranger, *Phys. Rev. B* **39**, 6227 (1991).
 - [21] K. Ismail, S. Washburn, and K. Y. Lee, *Appl. Phys. Lett.* **59**, 1998 (1991).
 - [22] D. Mailly, C. Chapalier, and A. Benoit, *Phys. Rev. Lett.* **70**, 2020 (1993).
 - [23] J. Liu, K. Ismail, K.Y. Lee, J.M. Hong, and S. Washburn, *Phys. Rev. B* **48**, 15148 (1993).
 - [24] J. Liu, K. Ismail, K.Y. Lee, J.M. Hong, and S. Washburn, *Phys. Rev. B* **50**, 17383 (1994).
 - [25] D. Loss, P. Goldbart, and A.V. Balatsky, *Phys. Rev. Lett.* **65**, 1655 (1990).
 - [26] A. Stern, *Phys. Rev. Lett.* **68**, 1022 (1992).
 - [27] A.G. Aronov and Y.B. Lyanda-Geller, *Phys. Rev. Lett.* **70**, 343 (1993).
 - [28] T.-Z. Qian and Z.-B. Su, *Phys. Rev. Lett.* **72**, 2311 (1994).
 - [29] Y.-S. Yi, T.-Z. Qian, and Z.-B. Su, *Phys. Rev. B* **55**, 10 631 (1997).

- [30] A.F. Morpurgo, J.P. Heida, T.M. Klapwijk, and B.J. van Wees, *Phys. Rev. Lett.* **80**, 1050 (1999).
- [31] J. Nitta, H. Takayanagi, and S. Calvet, *Microelectron. Eng.* **47**, 85 (1999).
- [32] J.B. Yau, E.P. de Poortere, and M. Shayegan, *Phys. Rev. Lett.* **88**, 146801 (2002).
- [33] M.J. Yang, C.H. Yang, K.A. Cheng, and Y.B. Lyanda-Geller, *cond-mat/0208260*.
- [34] M.V. Berry, *Proc. R.Soc. London A* **392**, 45 (1984).
- [35] In fact, the Aharonov-Bohm phase can be regarded as a special case of the Berry phase.
- [36] A. Fuhrer, S. Lüsher, T. Ihn, T. Heinzel, K. Ensslin, W. Wegscheider, and M. Bichler, *Nature* **413** 822 (2001).
- [37] S.M. Reimann and M. Manninen, *Rev. Mod. Phys.* **74**, 1283 (2002).
- [38] H. Pettersson, R.J. Warburton, A. Lorke, K. Karrai, J.P. Kotthaus, J.M. García, and P.M. Petroff, *Physica E* **6** 510 (2000).
- [39] R.J. Warburton, C. Schäfflein, D. Haft, F. Bickel, A. Lorke, K. Karrai, J.M. Garcia, W. Schoenfeld, and P.M. Petroff, *Nature* **405**, 926 (2000).
- [40] S. Pedersen, A. E. Hansen, A. Kristensen, C.B. Sørensen, and P. E. Lindelof, *Phys. Rev. B* **61**, 5457 (2000).
- [41] U.F. Keyser, C. Fühner, S. Borck, R.J. Haug, M. Bichler, G. Abstreiter, and W. Wegscheider, *Phys. Rev. Lett.* **90**, 196601 (2003).
- [42] P.A. Maksym, *Phys. Rev. B* **53**, 10871 (1996).
- [43] F. Calogero, *J. Math. Phys* **10**, 2191 (1969); **10**, 2197 (1969); **12**, 419 (1971).
- [44] B. Sutherland, *J. Math. Phys.* **12**, 246 (1971); **12** 251 (1971).
- [45] N.W. Ashcroft and N.D. Mermin, *Solid State Physics* (Saunders College, Philadelphia 1976).
- [46] M. Koskinen, M. Manninen, B. Mottelson, and S.M. Reimann, *Phys. Rev. B* **63**, 205323 (2001)
- [47] P. Koskinen, M. Koskinen, and M. Manninen, *Eur. Phys. J B* **28**, 483 (2002).
- [48] G. Herzberg, *Infrared and Raman Spectra of Polyatomic Molecules* (Van Nostrand, New York 1945).
- [49] M. Tinkham, *Group Theory and Quantum Mechanics* (McGraw-Hill, New York 1964).
- [50] D. Loss and P. Goldbart, *Phys. Rev. B* **43**, 13762 (1991).
- [51] M. Manninen, J. Mansikka-aho, and E. Hammarén, *Europhys. Lett.* **15**, 423 (1991).
- [52] R.M. Fye, M.J. Marints, D. Scalapino, J. Wagner, and W. Hanke, *Phys. Rev. B* **44**, 6909 (1991).
- [53] A.J. Schofield, J.M. Wheatley, and T. Xiang, *Phys. Rev. B* **44**, 8349 (1991).
- [54] F.V. Kusmartsev, *J. Phys.: Condens. Matt.* **3**, 3199 (1991).
- [55] N. Yu and M. Fowler, *Phys. Rev. B* **45**, 11795 (1992).
- [56] C.A. Stafford and A.J. Millis, *Phys. Rev. B* **48**, 1409 (1993).
- [57] F.V. Kusmartsev, *Phys. Rev. B* **52**, 14445 (1995).
- [58] M. Berciu and S. John, *Phys. Rev. B* **61**, 10015 (2000).
- [59] H.-P. Eckle, H. Johansson, and C.A. Stafford, *Phys. Rev. B* **87**, 016602 (2001).
- [60] R. E. Peierls, *Z. Phys.* **80**, 763 (1933).
- [61] A.L. Fetter and J.D. Walecka, *Quantum Theory of Many-Particle Systems* (McGraw-Hill, New York 1971).
- [62] G. Beni, T. Holstein and P. Pincus, *Phys. Rev. B* **8**, 312 (1973).
- [63] J. Bernasconi, M.J. Rice, W.R. Schneider and S. Strässler, *Phys. Rev. B* **12**, 1090 (1975).
- [64] D. Vollhardt in "Proceedings of the International School of Physics 'Enrico Fermi' Course CXXI", North Holland (1994).
- [65] B.S. Shastry and B. Sutherland, *Phys. Rev. Lett.* **65**, 243 (1990).
- [66] R. Kotlyar, C.A. Stafford, and S. Das Sarma, *Phys. Rev. B* **58**, 3989 (1998).
- [67] M. Karbach and G. Müller, *Computers in Physics* **11**, 36 (1997).
- [68] B.S. Shastry in *Correlation Effects in Low-Dimensional Electron Systems*, eds. A. Okiji and N. Kawakami (Springer, Berlin, 1994).
- [69] W.-C. Tan and J.C. Inkson, *Phys. Rev. B* **60**, 5626 (1999).
- [70] K. Niemelä, P. Pietiläinen, P. Hyvönen, and T. Chakraborty, *Europhys. Lett.* **36**, 533 (1996).
- [71] S.M. Reimann, M. Koskinen, and M. Manninen, *Phys. Rev. B* **59**, 1613 (1999)
- [72] M. Manninen, M. Koskinen, S.M. Reimann, and B. Mottelson, *Eur. Phys. J. D* **16**, 381 (2001).
- [73] S.M. Reimann, M. Koskinen, and M. Manninen, *Phys. Rev. B* **62**, 8108 (2000).
- [74] C. Yannouleas and U. Landman, *Phys. Rev. Lett.* **85**, 1726 (2000).
- [75] M. Dineykhon and R.G. Nazmitdinov, *Phys. Rev. B* **55**, 13707 (1997).
- [76] F. Bolton and U. Rößler, *Superlatt. Microstr.* **13**, 139 (1993).
- [77] M. Manninen, S. Viefers, M. Koskinen, and S.M. Reimann, *Phys. Rev. B* **64**, 245322 (2001).
- [78] T. Chakraborty, and P. Pietiläinen, *Phys. Rev. B* **50**, 8460 (1994).
- [79] F.V. Kusmartsev, J.F. Weisz, R. Kishore, and M. Takahashi, *Phys. Rev. B.* **49**, 16234 (1994).
- [80] P. Singha Deo, P. Koskinen, M. Koskinen, and M. Manninen, to be published.
- [81] D.M. Ceperley, in *Monte Carlo and Molecular Dynamics of Condensed Matter Systems*, Ed. K. Binder and G. Ciccotti (Editrice Compositori, Bologna, Italy, 1996).
- [82] F. Bolton, *Phys. Rev. Lett.* **73**, 158 (1994).
- [83] R. Egger, W. Häusler, C.H. Mak, and H. Grabert, *Phys. Rev. Lett.* **82** 3320 (1999).
- [84] A. Harju, V.A. Sverdlov, and R.M. Nieminen, *Phys. Rev. B* **59**, 5622 (1999).
- [85] J. Shumway, L. R. C. Fonseca, J. P. Leburton, R.M. Martin, and D. M. Ceperley, *Physica E* **8**, 260 (2000).
- [86] L. Colletti, F. Pederiva, E. Lipparini, C.J. Umrigar, *Eur. Phys. J. B* **27**, 385 (2002).
- [87] P. Borrmann and J. Harting, *Phys. Rev. Lett.* **86**, 3128 (2001).
- [88] F. Pederiva, A. Emperador, and E. Lipparini, *Phys. Rev. B* **66**, 165314 (2002).
- [89] Still quite recently there have been published several quantum Monte Carlo results which give the wrong total spin for as small system as the four electron quantum dot: F. Bolton, *Phys. Rev. B* **54**, 4780 (1996); F. Pederiva, C.J. Umrigar, and E. Lipparini, *Phys. Rev. B* **62**, 8120 (2000); J.O. Harting, Mülken and P. Borrmann, *Phys. Rev. B* **62**, 10207 (2000).
- [90] H. Häkkinen, J. Kolehmainen, M. Koskinen, P.O. Lipas and M. Manninen, *Phys. Rev. Lett.* **78**, 1034 (1997).
- [91] M. Koskinen, M. Manninen, and S.M. Reimann, *Phys. Rev. Lett.* **79**, 1389 (1997).

- [92] A. Emperador, M. Barranco, E. Lipparini, M. Pi, and Ll. Serra, Phys. Rev. B **59**, 15301 (1999).
- [93] A. Emperador, M. Pi, M. Barranco, and A. Lorke, Phys. Rev. B **62**, 4573 (2000).
- [94] S. Viefers, P.S. Deo, S.M. Reimann, M. Manninen, and M. Koskinen, Phys. Rev. B **62**, 10668 (2000).
- [95] A. Emperador, M. Pi, M. Barranco, and E. Lipparini, Phys. Rev. B **64**, 155304 (2001).
- [96] G. Vignale and M. Rasolt, Phys. Rev. B **37**, 10685 (1988).
- [97] J.M. Luttinger, Phys. Rev. **119**, 1153 (1960).
- [98] F.D.M. Haldane, J. Phys. C **14**, 2528 (1981).
- [99] R. Peierls, *Quantum theory of solids* (Oxford 1955).
- [100] M. Koskinen, unpublished.
- [101] H.-F. Cheung, Y. Gefen, E.K. Riedel, and W.-H. Shih, Phys. Rev. B **37**, 6050 (1988).
- [102] T. Chakraborty and P. Pietiläinen, Phys. Rev. B **52**, 1932 (1995).
- [103] V. Halonen, P. Pietiläinen, and T. Chakraborty, Europhys. Lett. **33**, 377 (1996).
- [104] H.-P. Eckle, H. Johannesson, and C.A. Stafford, J. Low Temp. Phys. **118**, 475 (2000).
- [105] F. von Oppen and E.K. Riedel, Phys. Rev. Lett. **66**, 84 (1991).
- [106] B.L. Altshuler, Y. Gefen, and Y. Imry, Phys. Rev. Lett. **66**, 88 (1991).
- [107] G. Montambaux, H. Bouchiat, D. Sigeti, and R. Friesner, Phys. Rev. B **42**, 7647 (1990).
- [108] V. Ambegaokar and U. Eckern, Phys. Rev. Lett. **65**, 381 (1990); *ibid* **67**, 3192 (1991).
- [109] Axel Müller-Groeling and Hans A. Weidenmüller, Phys. Rev. B **49**, 4752 (1994).